

See discussions, stats, and author profiles for this publication at: <https://www.researchgate.net/publication/236228119>

# Tumour targeting with radiometals for diagnosis and therapy

ARTICLE *in* CHEMICAL COMMUNICATIONS · APRIL 2013

Impact Factor: 6.83 · DOI: 10.1039/c3cc41554f · Source: PubMed

---

CITATIONS

47

---

READS

94

## 2 AUTHORS:



[Caterina F Ramogida](#)

TRIUMF

**11** PUBLICATIONS **138** CITATIONS

[SEE PROFILE](#)



[Chris Orvig](#)

University of British Columbia - Vancouver

**262** PUBLICATIONS **9,477** CITATIONS

[SEE PROFILE](#)

## Tumour targeting with radiometals for diagnosis and therapy

Cite this: *Chem. Commun.*, 2013, **49**, 4720

Caterina F. Ramogida<sup>ab</sup> and Chris Orvig<sup>\*a</sup>

Use of radiometals in nuclear oncology is a rapidly growing field and encompasses a broad spectrum of radiotracers for imaging *via* PET (positron emission tomography) or SPECT (single-photon emission computed tomography) and therapy *via*  $\alpha$ ,  $\beta^-$ , or Auger electron emission. This feature article opens with a brief introduction to the imaging and therapy modalities exploited in nuclear medicine, followed by a discussion of the multi-component strategy used in radiopharmaceutical development, known as the bifunctional chelate (BFC) method. The modular assembly is dissected into its individual components and each is discussed separately. The concepts and knowledge unique to metal-based designs are outlined, giving insight into how these radiopharmaceuticals are evaluated for use *in vivo*. Imaging nuclides  $^{64}\text{Cu}$ ,  $^{68}\text{Ga}$ ,  $^{86}\text{Y}$ ,  $^{89}\text{Zr}$ , and  $^{111}\text{In}$ , and therapeutic nuclides  $^{90}\text{Y}$ ,  $^{177}\text{Lu}$ ,  $^{225}\text{Ac}$ ,  $^{213}\text{Bi}$ ,  $^{188}\text{Re}$ , and  $^{212}\text{Pb}$  will be the focus herein. Finally, key examples have been extracted from the literature to give the reader a sense of breadth of the field.

Received 28th February 2013,  
Accepted 27th March 2013

DOI: 10.1039/c3cc41554f

[www.rsc.org/chemcomm](http://www.rsc.org/chemcomm)

### Introduction

Cancer is the leading cause of death worldwide, accounting for 7.6 million deaths in 2008, and an estimated 13.1 million deaths in 2030.<sup>1</sup> The burden of cancer can be reduced by early detection and early treatment management of patients, and in this regard nuclear imaging and therapy have made great

evolutions in clinical medicine. Nuclear medicine is a powerful tool with the ability to both image disease non-invasively and subsequently treat the diseased state without harming surrounding healthy tissue by injecting a radioactive isotope fused to a designer molecule that has the ability to transport the radionuclide specifically to the diseased tissue. Traditionally, 'organic' isotopes, such as  $^{18}\text{F}$ ,  $^{15}\text{O}$ ,  $^{13}\text{N}$ ,  $^{11}\text{C}$ , and  $^{131}\text{I}$  have been incorporated into nuclear medicine agents;<sup>2</sup> however, these agents were limited in availability and widespread use due to the need to incorporate these nuclides *via* covalent bond linkages into small organic drug mimics *via* lengthy and complex radiosyntheses

<sup>a</sup> Medicinal Inorganic Chemistry Group, Department of Chemistry, University of British Columbia, 2036 Main Mall, Vancouver, BC, Canada V6T 1Z1. E-mail: [orvig@chem.ubc.ca](mailto:orvig@chem.ubc.ca)

<sup>b</sup> TRIUMF, 4004 Wesbrook Mall, Vancouver, BC, Canada



Caterina F. Ramogida and Chris Orvig

Caterina began her chemistry career at Simon Fraser University in Burnaby, British Columbia, Canada, where she obtained an honours BSc (2010) while completing undergraduate research with Dr Tim Storr. She then began graduate studies as an NSERC scholar under the joint supervision of Drs Chris Orvig and Michael J. Adam where she has spent the past few years collaborating with Nordion researching PET imaging agents of gallium and copper isotopes. Chris Orvig is from Montréal; he completed his BSc (Hons. Chemistry) at McGill University and his doctorate (as a Natural Sciences and Engineering Research Council – NSERC – of Canada scholar) in technetium chemistry at M.I.T. with Alan Davison, FRS. After an NSERC postdoc with K. N. Raymond at Berkeley (1981–1983) and one year with Colin J. L. Lock at McMaster University, he joined the Department of Chemistry at the University of British Columbia in 1984. He is now Professor of Chemistry and Pharmaceutical Sciences, a Fellow of the Royal Society of Canada and a certified ski instructor.

**Table 1** Selected FDA-approved radiopharmaceuticals containing radiometals (excluding  $^{99m}\text{Tc}$ )<sup>3</sup>

Radiopharmaceutical	Trade name	Indications
$^{111}\text{In}$ capromab pendetide	ProstaScint <sup>®</sup>	SPECT – diagnostic imaging of prostate cancer
$^{111}\text{In}$ pentetreotide	Octreoscan <sup>™</sup>	SPECT – imaging of neuroendocrine tumours bearing somatostatin receptors
$^{153}\text{Sm}$ lexidronam	Quadramet <sup>®</sup>	$\beta^-$ Therapy – pain relief in patients with osteoblastic metastatic bone lesions
$^{90}\text{Y}$ ibritumomab tiuxetan	Zevalin <sup>®</sup>	$\beta^-$ Therapy – treatment of B-cell non-Hodgkin's lymphoma (NHL)

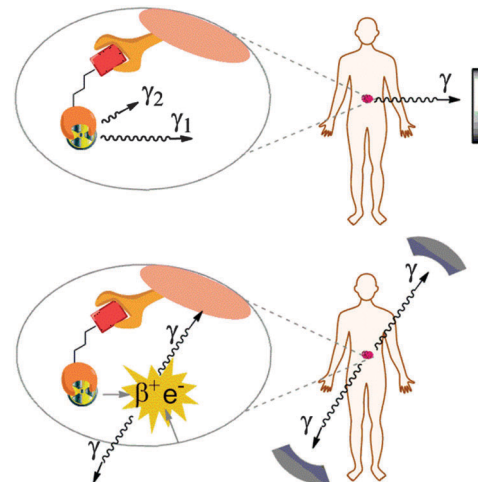
which can take valuable time sacrificing many short half-lives of radioactivity in the process. To overcome these shortcomings, much effort has been made towards the development of metallic radionuclides with varying production methods, radioactive decay schemes, and half-lives that make them attractive for incorporation into a radiopharmaceutical. In 2012, of the 41 FDA-approved radiopharmaceuticals on the market, 14 employ non-metallic isotopes ( $^{18}\text{F}$ ,  $^{11}\text{C}$ ,  $^{14}\text{C}$ ,  $^{123}\text{I}$ ,  $^{125}\text{I}$ ,  $^{131}\text{I}$ ,  $^{13}\text{N}$ ) and the remainder rely on the use of metallic isotopes for their source of radiation (Table 1).<sup>3</sup> The most prevalent metal used in nuclear medicine,  $^{99m}\text{Tc}$ , is a  $\gamma$  emitter used extensively in single-photon emission computed tomography (SPECT).  $^{99m}\text{Tc}$  is incorporated into 16 FDA-approved radiopharmaceuticals, and has been widely discussed and reviewed in the literature.<sup>4,5</sup> The recent global supply shortage of  $^{99}\text{Mo}$ , the parent isotope of  $^{99m}\text{Tc}$ , due to shut down of the National Research Universal reactor in Chalk River Laboratory in Ontario, Canada, has fostered an increased interest in exploring radiopharmaceuticals using other radiometals.

## Imaging

The ability to image cancers and monitor the progression of the disease non-invasively has become common practice in clinical medicine, proving vital to patient survival. Two imaging modalities are used extensively in nuclear medicine: single-photon emission computed tomography (SPECT) and positron emission tomography (PET). Both modalities require the introduction of a radioactive nuclide into the patient; the radioactivity will be attached to some targeting moiety that will deliver the radionuclide to the tumour site. The radiative emissions will be detected by cameras and ultimately converted into a 3D image visualising the accumulation of radioactivity in the body, coinciding with the localization of the tumour. The use of SPECT and PET in the clinic depends on a variety of factors such as cost, sensitivity and resolution of the technique, and availability of an appropriate radionuclide. Some important properties of each imaging modality are discussed below.

### Single-photon emission computed tomography (SPECT)

The eldest of the two techniques, SPECT requires a  $\gamma$ -emitting radionuclide whose emissions are recorded by detector cameras (Fig. 1). The discovery of the  $\gamma$ -emitter  $^{99m}\text{Tc}$  (in 1937) and introduction of the  $^{99}\text{Mo}/^{99m}\text{Tc}$  generator system used in the production of the isotope in the 1960's led to widespread use of  $^{99m}\text{Tc}$ -labelled agents in clinical SPECT imaging, and today this generator and radionuclide are still the workhorses of medical imaging, used in about 70–80% of all radio-diagnostic scans.<sup>6,7</sup> There have been many extensive reviews on  $^{99m}\text{Tc}$ .<sup>4,5</sup>

**Fig. 1** Depiction of SPECT imaging (top) and PET imaging (bottom).

Industrially,  $\gamma$  camera/detectors are designed for specific energy windows (generally 100–250 keV),<sup>8</sup> and  $\gamma$  rays with energies outside this range will produce poor image quality. As a consequence, SPECT radionuclides should have a  $\gamma$  decay energy within this range to be clinically useful. Typically, SPECT systems can detect radiotracers within the body at concentrations of about  $10^{-6}$  M;<sup>9</sup> however, more modern SPECT instruments have shown sensitivity down to nanomolar and even picomolar levels.<sup>10</sup>

### Positron-emission tomography (PET)

As implied by its name, PET requires a  $\beta^+$ -emitting radionuclide. As the nuclide decays it ejects a  $\beta^+$  from its nucleus; the  $\beta^+$  will travel a short distance before it collides with an electron, and the two annihilate to release two  $180^\circ$  opposed 511 keV  $\gamma$  rays (Fig. 1). The  $\gamma$  rays will travel in this direction until they strike the PET scanner coincidence detectors (arranged in a circular array); the output is generated only when two coincidence detectors are triggered simultaneously (the coincidence time window is approximately 5–15 ns).<sup>11</sup>

The first industrial positron emission tomograph arrived in 1975,<sup>12</sup> and for many years PET imaging agents were dominated by short half-life isotopes  $^{18}\text{F}$ ,  $^{15}\text{O}$ ,  $^{13}\text{N}$ , and  $^{11}\text{C}$ , whose production relied upon an on-site cyclotron. Not only did the need for an on-site cyclotron make PET an expensive imaging modality, but the short half-lives of the organic nuclides (122 s to 109 min) limited the use of PET for imaging biological processes that occurred over a short time scale. Today,  $^{18}\text{F}$  ( $t_{1/2} = 109$  min) dominates the field of PET imaging, and is readily available daily from commercial sources obviating the need for an on-site cyclotron.

Nonetheless, tremendous effort has been made towards the production of  $\beta^+$  emitting radioisotopes of metals such as Ga, Y, Zr and Cu,<sup>8,13</sup> that have varying half-lives and can circumvent some of the synthetic limitations still associated with incorporating organic  $\beta^+$  emitting nuclides into small drug mimics. Despite these efforts, there is currently no FDA-approved metal-based PET imaging agent; however, many are in early to late stage clinical trials.

Compared to its single-photon analogue, PET exhibits higher resolution (2–4 mm or lower compared to 6–8 mm for SPECT) and higher sensitivities (up to  $\sim 10^{-12}$  M, compared to  $10^{-6}$  M for SPECT).<sup>13</sup> The resolution and sensitivity of PET is tied to the intrinsic properties of  $\beta^+$  emission. Firstly, the resolution depends on the initial distance the  $\beta^+$  travels before annihilation; this distance is dependent on the energy of decay. Hence, lower energy  $\beta^+$  emission is more desirable in PET in order to give better resolution. Secondly, high sensitivity is a result of the coincidence detection of two  $\gamma$ -rays. Despite the advantages of PET imaging, SPECT is more widely used in the clinic, perhaps only because it is a more established technique.

## Therapy

Radioactivity used to target and kill cancer cells is often termed radiotherapy, and when conjugated to a large monoclonal antibody is called radioimmunotherapy (RIT). These therapeutic radiopharmaceuticals are similar in construction to their nuclear imaging analogues. An unstable radionuclide which decays *via* emission of high-energy ionizing radiation is attached to a targeting moiety that will deliver the radiation dose specifically to the cancer cells; from here the emission deposits its energy in the surrounding tissue, causing cell death. In order to kill the cell, the ionization must cause DNA double-strand helix breaks that are non-repairable.<sup>14</sup>

Emissions of therapeutic nuclides should contain mainly non-penetrating radiation so that a damaging and highly-localised dose can be delivered to the diseased tissue without causing harm to surrounding healthy tissue.<sup>6</sup> Emitters of beta particles ( $\beta^-$ ), alpha particles ( $\alpha$ ), and Auger electrons may be used for radiotherapy. Varying physical properties and effects on tissue are associated with each type of radiation, and must be matched appropriately with their intended biological target. The linear energy transfer (LET) value is used to quantify the amount of energy that is transferred from ionizing radiation to soft tissue, typically expressed in kiloelectron volts per micrometer of track length in tissue ( $\text{keV } \mu\text{m}^{-1}$ ). Emissions of high LET will dissipate their energy in tissue close to where the nuclide is deposited (shorter 'effective range'), making them effective for treating small tumours and micrometastases. Conversely, emissions of low LET will deposit their energy through a larger range in tissue suggesting cell damage can occur many cell lengths away from where the nuclide is deposited; these emissions are more appropriately matched for treating larger or poorly vascularized tumours<sup>15,16</sup> (Table 2). It is also worth noting that  $\beta^+$  emission is capable of being used therapeutically due to its high LET value if given at an appropriate therapeutic dose.

**Table 2** Type of radiation for radiotherapy with corresponding path length and decay energy

Radiation	Typical range in biological tissue <sup>a</sup>	Typical energy of decay
Auger electrons	1–20 $\mu\text{m}$ ( $<1$ cell diameter)	$\sim 1$ –10 keV
$\alpha$ particles	40–100 $\mu\text{m}$ ( $<10$ cell diameters)	5–8 MeV
$\beta^-$ particles	0.5–10 mm (50–1000 cell diameters)	0.1–2.2 MeV

<sup>a</sup> Based on 10  $\mu\text{m}$  average cell diameter.

## Beta-particles ( $\beta^-$ )

Traditionally,  $\beta^-$  particle emitters have most commonly been exploited for radiotherapy.  $\beta^-$  particles have a low LET ( $0.2 \text{ keV } \mu\text{m}^{-1}$ ) allowing the particles to reach spans of approximately 50 cell diameters<sup>15</sup> which makes  $\beta^-$  emitting nuclides appropriate for treating larger or poorly vascularized tumours. Conversely, using a  $\beta^-$  emitter to treat small tumours may cause damage to neighbouring healthy cells, a potential disadvantage.<sup>15</sup>

## Alpha-particles ( $\alpha$ )

Alpha particles have a very short path length ( $<100 \mu\text{m}$ ) corresponding to a very high LET (typically about  $100 \text{ keV } \mu\text{m}^{-1}$ ),<sup>16</sup> the short range and high LET of  $\alpha$  particles renders their emitters ideal for treating small tumours since they are only effective over a few cell diameters. In addition, the short range in biological tissue offers less radiotoxicity and more favourable dosimetry profiles for surrounding healthy tissues.<sup>6</sup>

## Auger electrons

Most Auger electron emitters have low energies ( $<500 \text{ eV}$ ) and the smallest range (several nanometers) in biological tissue of all the other ionizing radiations discussed.<sup>17</sup> This makes them effective only when the radionuclide is localised in the cell nucleus. With a highly-localised energy deposition, Auger electron emissions have the potential to provide an effective cell-killing dose to the target site with minimal chance of damage to surrounding cells.<sup>18</sup>

## Construction and evaluation of metalloradiopharmaceuticals

### Bifunctional chelate (BFC) method

The nature of radiometals in radiopharmaceuticals lends itself to an interdisciplinary approach requiring knowledge of coordination chemistry, thermodynamics and kinetics, synthetic chemistry, radiochemistry, and biology/physiology. The basis for a good inorganic radiopharmaceutical is a bifunctional chelate (BFC). The BFC has the dual function of binding a radiometal and incorporating a point of derivatisation for attachment of a biomolecule/targeting vector (the moiety that will introduce site-specific delivery). In general, a fully functional metal-based radiopharmaceutical will contain four components: (1) targeting vector, (2) radiometal (imaging handle or therapeutic effect), (3) chelate (required to bind and fully sequester the radiometal), and (4) linker (connects the chelate to the biomolecule). The targeting vector is generally a biomolecule of interest

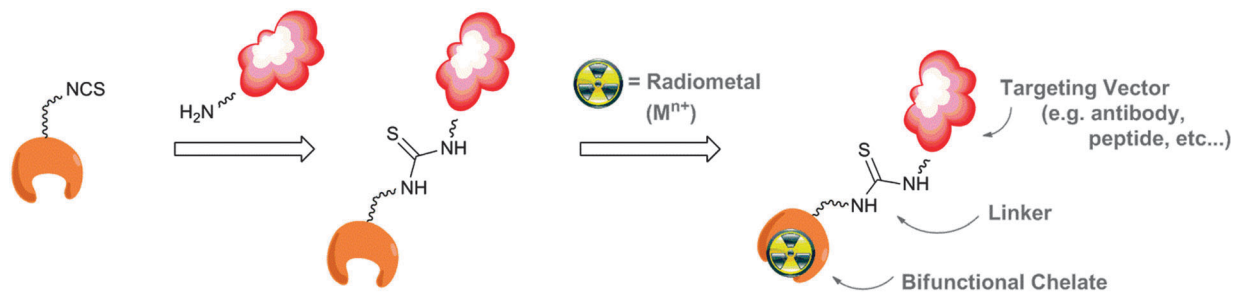


Fig. 2 Example of the bifunctional chelate (BFC) method employed in metal-based radiopharmaceuticals.

(e.g. peptide, antibody, antibody fragment) that exhibits strong binding affinity for over-expressed tumour surface receptors; these are the vehicles that transport the radioactivity specifically to the tumour. The appropriate radiometal is chosen based on the radiopharmaceutical's intended purpose;  $\gamma$ - or  $\beta^+$ -emitting radionuclides for imaging,  $\alpha$ -,  $\beta^-$ -, or Auger electron emitters for therapy. Choice of an appropriate BFC is based on the best-fit of the radiometal governed by preferences in coordination chemistry and donor-ability of the ligand in order to form a stable and inert metal-chelate complex. Finally, the linker is used to connect the chelate to the targeting vector. The linker should be stable under physiological conditions and must not significantly compromise the binding affinity or specificity of the biovector or the metal-complexation performance of the chelator. The BFC method is particularly attractive because all steps of the long synthetic manipulation of the chelate, linker, and biomolecule is executed before the radionuclide is added in the last step (Fig. 2), saving many half-lives of radioactivity.

Components must be carefully chosen when designing a successful radiopharmaceutical so as to mutually complement each other in order to work as a unified agent. For example, matching the biological half-life of the biomolecule with the radioactive half-life of the nuclide is crucial. In general, radiometals with long half-lives are best matched to biomolecules with long biological half-lives (such as antibodies) that may take hours or days to circulate the blood and accumulate at the tumour site, and short half-life isotopes are best matched with biomolecules that have short biological half-lives (such as small molecules or peptides) that rapidly circulate the blood and accumulate at the tumour site at a time frame that is comparable with the short radiological half-life of the nuclide.

Exceptions to the BFC method, such as the 'integrated approach', are also used extensively in radiopharmaceutical design and have been discussed elsewhere.<sup>19</sup> The metal-chelate complex Cu(II)-ATSM (Cu(II)-diacetyl-bis( $N^4$ -methylthiosemicarbazone))<sup>20</sup> (Fig. 3) is an archetypal example of an exception to the BFC method. ATSM and its analogues have been labelled

with several copper isotopes, and show a striking ability to treat or image hypoxic cancer tissue. The ability to specifically target and become entrapped in hypoxic cells is rooted in the complex's biochemical interaction with cells, and redox chemistry,<sup>20,21</sup> and is not dependent on a biomolecule as a means of tumour-specific transportation.

### Properties of a good radiopharmaceutical-methods for evaluation of a radiopharmaceutical

Due to the 'multi-component' nature of metal-based radiopharmaceuticals, there are many properties that must be evaluated when assessing the potential of a radiopharmaceutical. Some important considerations are outlined below.

First and foremost, the metal-chelate complex must be kinetically inert and thermodynamically stable. The chelator must be a 'good fit' for the metal of choice; there are many commonly used and emerging chelates that have been used for a variety of radiometals with varying degrees of success (*vide infra*). Typically, the thermodynamic stability of the metal-chelate complex is measured *via* potentiometric titration or UV-Vis spectroscopy to calculate values of  $\log K_{ML}$  and  $pM$  which are used to quantify the binding affinity of a particular metal-chelator pair, where a higher value signifies a stronger affinity between metal and chelate. More important than thermodynamic stability is the kinetic inertness of the metal-ligand complex *in vivo*.<sup>8</sup> There are many endogenous metal binding proteins in plasma that can compete with the chelate for the metal, thus the metal must be bound sufficiently tightly to inhibit transchelation of the metal to these proteins. Specifically, superoxide dismutase has a strong affinity for copper, and the iron binding protein transferrin has high binding affinity for both Ga(III) and In(III). In addition, highly charged ions such as Y(III) and Zr(IV) tend to accumulate in the bone.<sup>22,23</sup> Kinetic inertness of the metal-ligand complexes is often estimated experimentally by *in vitro* competition or challenge assays against excess metal-free protein, or blood serum. Caution must be taken when interpreting *in vitro* stability data, as *in vitro* studies rarely accurately predict *in vivo* stability of the radiopharmaceutical.

In addition to a thermodynamically stable and kinetically inert metal-chelate complex, appropriate complexation kinetics of the radioisotope are required under radiochemical conditions such as low concentrations, mild temperatures, and minimal time. The goal is to introduce as much radioactivity into the chelate-bioconjugate as possible, while protecting the integrity of the biomolecule and preserving the radioactivity of the nuclide

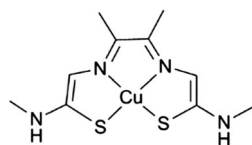


Fig. 3 Cu(II)-ATSM.



which decays over time. These characteristics are expressed in radiochemical yield (% RCY), the percent of nuclide which is bound to the chelate, and specific activity (mCi/mg), the amount of activity introduced per mg of compound.

Ultimately, the usefulness of any radiopharmaceutical is governed by the distribution of the agent in the body, *i.e.* biodistribution. Ideally, the agent will circulate in the blood and accumulate only in the tumour tissue that is meant to be imaged or given a therapeutic dose of radiation. Excess radiopharmaceutical that has not accumulated in the tumour tissue should be excreted to eliminate a background signal (for imaging), and reduce damage to surrounding healthy tissue (for therapy). This target accumulation and nonspecific clearance should occur at a time-scale which is matched with the half-life of the isotope. Biodistribution studies are done to determine the quantity and dose of radioactivity delivered to different organs in small animal models. Data are collected at different time points post-injection, and units are typically expressed in percent injected dose per gram of tissue (%ID/g); a high %ID/g value should be observed for the tumour, and low doses in all other tissues.

## Radiometals

Dozens of radiometals have been considered for use in nuclear imaging or therapy, here we will focus on the radioisotopes that have garnered the most attention and have the greatest potential. The coordination and aqueous chemistry of the metal ion(s) should be well-known in order to choose the appropriate chelate to form a stable, kinetically inert radiometal complex. In addition, the radionuclide should be produced in high chemical purity with high specific activity and should be readily available to hospitals and research institutions.<sup>7,24</sup> Finally, the radiometal should have favourable decay characteristics: the desired decay emission should have a high branching ratio, appropriate energy of decay, and half-life to fit its intended purpose. Also, when choosing a radiometal for therapeutic purposes it is often favourable for the nuclide to have an imageable decay radiation (such as  $\gamma$  or  $\beta^+$ ) in addition to the therapeutic emission, so there is means to determine the distribution of the radiopharmaceutical non-invasively for dosimetry studies. Discrepancies in physical decay data of relevant radiometals can be found throughout the literature and have been recently documented<sup>25</sup> and data provided herein (Tables 3 and 4) should be taken as approximate.

### Radiometals for PET and SPECT

**Copper-64 (PET).**  $^{64}\text{Cu}$  ( $t_{1/2} = 12.7$  h) decays *via*  $\beta^+$  emission (18%) with a maximum  $\beta^+$  energy of 653 keV, the remainder

decays *via* electron capture (43%) and  $\beta^-$  emission (39%).<sup>8,9</sup> Despite its relatively low  $\beta^+$  yield,  $^{64}\text{Cu}$  is a popular isotope used in development of PET imaging agents, and has been proposed as a dual imaging/therapy agent because of its accompanying  $\beta^-$  emission (0.579 MeV). Due to its intermediate half-life,  $^{64}\text{Cu}$ -based radiopharmaceuticals can be used with small molecules, peptides or antibodies.<sup>6,9</sup>  $^{64}\text{Cu}$  can also provide a matched element PET imaging pair with the pure  $\beta^-$  emitter  $^{67}\text{Cu}$  ( $t_{1/2} = 62$  h), despite the fact the decay of  $^{67}\text{Cu}$  gives rise to three  $\gamma$  rays suitable for SPECT imaging.<sup>26</sup> There are currently four clinical trials of various  $^{64}\text{Cu}$  radiopharmaceuticals underway,<sup>27</sup> three of which incorporate a monoclonal antibody as the targeting vector of choice.<sup>27</sup>  $^{64}\text{Cu}$  is commercially available and can be produced in a biomedical cyclotron *via* proton irradiation of enriched  $^{64}\text{Ni}$  at 12 MeV *via* the  $^{64}\text{Ni}(p,n)^{64}\text{Cu}$  reaction.<sup>6,28</sup>

In aqueous media, copper is predominantly in its +2 oxidation state, with a  $3d^9$  electronic configuration and is susceptible to Jahn–Teller distortion.  $\text{Cu(II)}$  is classified as a borderline hard cation, hence it has high affinity for borderline donor atoms such as nitrogen.<sup>8,28</sup> The coordination number (CN) of  $\text{Cu(II)}$  ranges between 4–6 with an ionic radius of 57–73 pm.<sup>29</sup>  $\text{Cu(II)}$  and its complexes are susceptible to reduction *in vivo* (redox potentials of cellular reductases range between –200 and –400 mV *versus* NHE). The  $\text{Cu(II)}/\text{Cu(I)}$  reduction has been suggested to be a viable cause of radiocopper loss since  $3d^{10}$   $\text{Cu(I)}$  is much more labile to ligand exchange; hence, kinetic inertness of the copper-complex is of utmost importance in radiopharmaceutical design.<sup>6,30</sup>

**Gallium-68 (PET).**  $^{68}\text{Ga}$  ( $t_{1/2} = 67.7$  min) is a  $\beta^+$  emitter (89%) of maximum  $\beta^+$  energy 1.9 MeV.<sup>8</sup>  $^{68}\text{Ga}$ -based radiopharmaceuticals are typically matched with biovectors that can localize quickly, such as small molecules, peptides, and antibody fragments.<sup>7,31</sup>  $^{68}\text{Ga}$  is an attractive PET nuclide because it is produced in a commercially available  $^{68}\text{Ge}/^{68}\text{Ga}$  generator system, and decays predominantly *via*  $\beta^+$  emission. The half-life of the parent  $^{68}\text{Ge}$  ( $t_{1/2} = 270$  d) allows the generator to be used for up to 1 year, with two or three elutions per day, obviating the need for an on-site cyclotron.<sup>31</sup> The  $^{68}\text{Ge}/^{68}\text{Ga}$  generator system is not yet FDA-approved, this deficiency is reflected in the lack of any  $^{68}\text{Ga}$  FDA-approved imaging agents on the market; however, four clinical trials of varying  $^{68}\text{Ga}$ -labelled peptides or antibody fragments are on-going.<sup>27</sup>

In aqueous solution, gallium is exclusively in its +3 oxidation state, and free hydrated  $[\text{Ga}(\text{H}_2\text{O})_6]^{3+}$  is stable only under acidic conditions.<sup>8</sup> Gallium has a strong affinity for hydroxide ions, and when the pH of solution is raised above  $\sim 4$ , insoluble  $\text{Ga}(\text{OH})_3$  begins to form. At  $\text{pH} > 7$   $[\text{Ga}(\text{H}_2\text{O})_6]^{3+}$  hydrolyses to the gallate anion  $[\text{Ga}(\text{OH})_4]^-$  which may result in demetallation

**Table 3** Selected radiometals for imaging and relevant physical decay data

Nuclide	Half-life	Emission (branching ratio)	$E_{\text{max}}$	$E_{\text{avg}}$	Production	Modality	Ref.
$^{64}\text{Cu}$	12.7 h	$\beta^+$ (18%)	653 keV	278 keV	Cyclotron, $^{64}\text{Ni}(p,n)^{64}\text{Cu}$	PET	6, 8, 13
$^{68}\text{Ga}$	67.7 m	$\beta^+$ (89%)	1.899 MeV	836 keV	Generator, $^{68}\text{Ge}/^{68}\text{Ga}$	PET	6, 12, 13
$^{86}\text{Y}$	14.7 h	$\beta^+$ (32%)	1.221 MeV	535 keV	Cyclotron, $^{86}\text{Sr}(p,n)^{86}\text{Y}$	PET	6, 7, 13
$^{89}\text{Zr}$	3.3 d	$\beta^+$ (23%)	902 keV	396 keV	Cyclotron, $^{89}\text{Y}(p,n)^{89}\text{Zr}$	PET	6, 13
$^{111}\text{In}$	2.8 d	EC (100%)		171 keV	Cyclotron, $^{111}\text{Cd}(p,n)^{111\text{m,g}}\text{In}$	SPECT	6, 7
				245 keV	$^{112}\text{Cd}(p,2n)^{111\text{m,g}}\text{In}$		

**Table 4** Selected radiometals for radiotherapy and relevant physical decay data

Nuclide	Half-life	Emission (branching ratio)	$E_{\max}$	$E_{\text{avg}}$	Production	Comment	Ref.
$^{67}\text{Ga}$	3.3 d	Auger (4.7 yield <sup>a</sup> )		6.26 keV	$^{68}\text{Zn}(\text{p},2\text{n})^{67}\text{Ga}$	Imaging $\gamma$ radiation (93, 185 & 300 keV)	15, 17, 50
$^{111}\text{In}$	2.8 d	Auger (14.7 yield <sup>a</sup> )		6.75 keV	Cyclotron, $^{111}\text{Cd}(\text{p},\text{n})^{111\text{m,g}}\text{In}$	Imaging $\gamma$ radiation (171 & 245 keV)	17
$^{201}\text{Tl}$	3.0 d	Auger (36.9 yield <sup>a</sup> )		15.27 keV	$^{112}\text{Cd}(\text{p},2\text{n})^{111\text{m,g}}\text{In}$ $^{203}\text{Tl}(\text{p},3\text{n})^{201}\text{Pb}^{201}\text{Tl}$	Imaging $\gamma$ radiation (167 & 135 keV)	15, 17
$^{203}\text{Pb}$	2.2 d	Auger (23.3 yield <sup>a</sup> )		11.63 keV	$^{203}\text{Tl}(\text{p},\text{n})^{203}\text{Pb}$ $^{203}\text{Tl}(\text{d},2\text{n})^{203}\text{Pb}$	Imaging $\gamma$ radiation (279 & 401 keV)	15, 17
$^{213}\text{Bi}$	45.7 m	$\alpha$ (2%) $\beta^-$ (98%)	5.87 MeV $\alpha$ 5.55 MeV $\alpha$		Generator, $^{225}\text{Ac}/^{213}\text{Bi}$	Imaging $\gamma$ radiation (440 keV)	6, 15, 50
$^{225}\text{Ac}$	10.0 d	$\alpha$ (100%)	5.83 MeV $\alpha$ 5.79 MeV $\alpha$ 5.73 MeV $\alpha$		$n$ -Capture of $^{232}\text{Th} \rightarrow ^{233}\text{U} \rightarrow ^{225}\text{Ac}$	Imaging $\gamma$ radiation (86 & 440 keV)	15, 50, 51
$^{90}\text{Y}$	2.7 d	$\beta^-$ (100%)	2.27 MeV $\beta^-$	935 keV $\beta^-$	Generator, $^{90}\text{Sr}/^{90}\text{Y}$	No imaging radiation	7, 15, 35, 50
$^{177}\text{Lu}$	6.6 d	$\beta^-$ (100%)	497 keV $\beta^-$ 384 keV $\beta^-$ 176 keV $\beta^-$		$^{176}\text{Lu}(\text{n},\gamma)^{177}\text{Lu}$	Imaging $\gamma$ radiation (208 & 113 keV)	15, 50
$^{186}\text{Re}$	3.7 d	$\beta^-$ (91%)	1.02 MeV $\beta^-$		$^{185}\text{Re}(\text{n},\gamma)^{186}\text{Re}$	Imaging $\gamma$ radiation (137 keV)	35, 37
$^{188}\text{Re}$	17.0 h	$\beta^-$ (100%)	2.10 MeV $\beta^-$		Generator, $^{188}\text{W}/^{188}\text{Re}$	Imaging $\gamma$ radiation (155 keV)	37, 38
$^{212}\text{Pb}$	10.2 h	$\beta^-$ (100%)	570 keV $\beta^-$ 6.09 MeV $\alpha^b$ 6.05 MeV $\alpha^b$		Generator, $^{224}\text{Ra}/^{212}\text{Pb}$	Imaging $\gamma$ radiation	48

<sup>a</sup> Auger yield = mean number of Auger electrons per decay. <sup>b</sup> Decay from  $^{212}\text{Bi}$  daughter.

of its complexes.<sup>8</sup>  $\text{Ga}(\text{III})$  is a small and highly charged cation with ionic radius of 47–62 pm (CN 4–6),<sup>29</sup> and can be classified as a hard acidic cation that prefers hard donor ligands such as anionic oxygen, and nitrogen.  $\text{Ga}(\text{III})$  can form 3–6 coordinate complexes; however, most successful  $\text{Ga}(\text{III})$  ligands are hexadentate, forming (distorted) octahedral complexes, since they are known to be thermodynamically stable and kinetically inert.<sup>8,13,24</sup>

**Yttrium-86 (PET).** With a half-life of 14.7 h  $^{86}\text{Y}$  decays *via* the emission of a relatively high energy  $\beta^+$  particle (32%, 1.2 MeV), and  $\gamma$  emission (68%, 1.08 MeV).<sup>6,13</sup>  $^{86}\text{Y}$  is a proposed PET nuclide since it can be used as an imaging surrogate for estimation of the pharmacokinetics and biodistribution of pure  $\beta^-$  emitter  $^{90}\text{Y}$ . The advantage of using  $^{86}\text{Y}$  as an imaging surrogate, as opposed to other surrogates such as  $^{111}\text{In}$  or  $^{89}\text{Zr}$ , is that identical chelate-bioconjugates can be used in parallel since  $^{86}\text{Y}$  and  $^{90}\text{Y}$  share the same chemistry.<sup>32</sup> Currently, no FDA-approved or clinical trials of  $^{86}\text{Y}$  agents exist. High specific activity  $^{86}\text{Y}$  can be produced in a medical cyclotron by irradiating  $\text{SrCO}_3$  or  $\text{SrO}$  with 8–15 MeV protons *via* the  $^{86}\text{Sr}(\text{p},\text{n})^{86}\text{Y}$  reaction.<sup>8</sup>

Yttrium is a large second row pre-transition metal which prefers the +3 oxidation state; with ionic radius of 90–108 pm (CN 6–9),<sup>29</sup> it can achieve coordination numbers as high as 10.  $\text{Y}(\text{III})$  is considered a hard acidic cation (harder than  $\text{Ga}(\text{III})$  or  $\text{In}(\text{III})$ ), and prefers hard donor atoms such as oxygen and nitrogen.<sup>8</sup>

**Zirconium-89 (PET).**  $^{89}\text{Zr}$  ( $t_{1/2} = 78.4$  h) is a  $\beta^+$  emitter (23%, 902 keV) with an ideal half-life for labelling antibodies in immuno-PET imaging.<sup>33</sup> Three  $^{89}\text{Zr}$ -labelled antibodies are in different phases of clinical trials.<sup>27</sup>  $^{89}\text{Zr}$  can be produced through a  $^{89}\text{Y}(\text{p},\text{n})^{89}\text{Zr}$  reaction upon irradiation of natural yttrium foil with a 14–14.5 MeV proton beam.<sup>7</sup>

A group 4 second row transition metal, zirconium forms an extremely acidic hydrated  $\text{Zr}^{4+}$  cation with a small radius of 59–89 pm (CN 4–9).<sup>29</sup> Hydrated  $\text{Zr}(\text{IV})$  likely only exists in extremely dilute and acidic solutions, and tends to form multiple monomeric and polynuclear oxo/hydroxyl species in basic media.<sup>8</sup> The extremely hard character of  $\text{Zr}(\text{IV})$  means it prefers to form complexes with multidentate ligands with hard donor atoms such as anionic oxygen from carboxylic acid or phosphinic acid residues, and prefers to form octadentate complexes.<sup>8,34</sup>

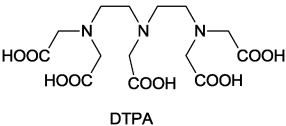
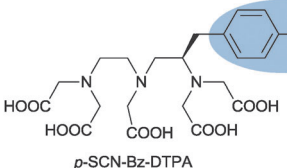
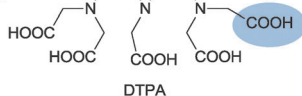
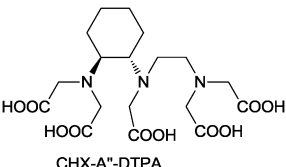
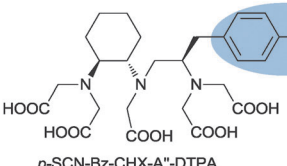
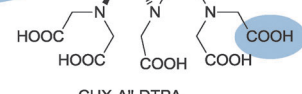
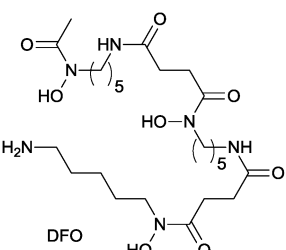
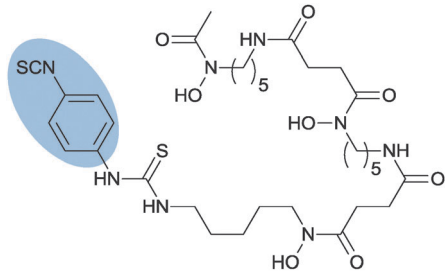
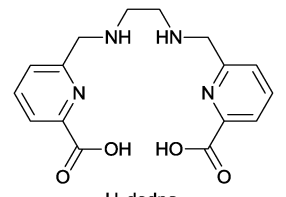
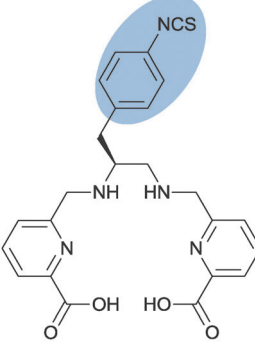
**Indium-111 (SPECT).**  $^{111}\text{In}$  is the next most popular metallic SPECT radioisotope after  $^{99\text{m}}\text{Tc}$ . With a half-life of 2.8 days,  $^{111}\text{In}$  decays *via* electron capture (100%) by emission of two  $\gamma$  rays of energies 171 and 245 keV.<sup>8</sup> Its half-life is long enough for incorporation into antibody-based radiopharmaceuticals, and  $^{111}\text{In}$  has been successfully introduced into two FDA-approved pharmaceuticals, sold under the trade names Octreoscan<sup>TM</sup> and ProstaScint<sup>®</sup>. In addition there are several  $^{111}\text{In}$ -labelled radiopharmaceuticals in early to late stage clinical trials.<sup>27</sup>  $^{111}\text{In}$  is produced commercially *via* the  $^{111}\text{Cd}(\text{p},\text{n})^{111}\text{In}$  reaction or the  $^{112}\text{Cd}(\text{p},2\text{n})^{111}\text{In}$  reaction, where natural cadmium is used as the target in both cases and irradiated with a proton beam,  $^{111}\text{In}$  is subsequently removed from the target by ion exchange or solvent extractions.<sup>8</sup>

Indium is a group 13 element, and in aerobic aqueous media is only stable in the +3 oxidation state; its size (62–92 pm for CN 4–8 respectively<sup>29</sup>) means  $\text{In}(\text{III})$  can reach coordination numbers of 7–8. It is a fairly hard acidic cation and consequently prefers chelators with hard donor atoms.<sup>8</sup>

## Radiometals for therapy

**Yttrium-90 ( $\beta^-$ ).**  $^{90}\text{Y}$  is a widely studied radiometal for  $\beta^-$  therapy. With a half-life of 64 hours, it decays solely *via*  $\beta^-$  emission (100%) with a maximum energy of 2.27 MeV to form

**Table 5** Selected acyclic chelators and their bifunctional analogues (coupling moiety highlighted in blue)

Chelate	Native donor set	Metal ions (log $K_{ML}$ )	Bifunctional analogues
 DTPA	$N_3O_5$	Cu(II) (21.4) <sup>a</sup> Ga(III) (25.5) <sup>a</sup> In(III) (29.5) <sup>a</sup> Y(III) (22.0) <sup>a</sup> Zr(IV) (35.8) <sup>a</sup> Bi(III) (35.6) <sup>b</sup>	 p-SCN-Bz-DTPA  DTPA
 CHX-A''-DTPA	$N_3O_5$	In(III) Bi(III) Ac(III) Lu(III) Y(III)	 p-SCN-Bz-CHX-A''-DTPA  CHX-A''-DTPA
 DFO	$O_6$	Ga(III) (28.6) <sup>a</sup> Zr(IV)	 p-SCN-Bz-DFO
 H <sub>2</sub> dedpa	$N_4O_2$	Ga(III) (28.1) <sup>c</sup>	 p-SCN-Bz-H <sub>2</sub> dedpa

<sup>a</sup> Ref. 8. <sup>b</sup> Ref. 46. <sup>c</sup> Ref. 53.

<sup>90</sup>Zr after decay.<sup>35</sup> <sup>90</sup>Y is an attractive radionuclide for therapy because it has a long enough half-life to be transported for clinical use and can be coupled to large targeting vectors such as antibodies; furthermore, the lack of  $\gamma$ -emission reduces the radiation dose to clinicians and patients.<sup>8</sup> The FDA-approved agent sold under the trade name Zevalin<sup>®</sup> is a <sup>90</sup>Y-labelled monoclonal antibody in  $\beta^-$  therapy of B-cell non-Hodgkin's lymphoma. The success of Zevalin<sup>®</sup> has sparked an increase in the number of <sup>90</sup>Y clinical trials, most of which are small variations or combination therapy protocols of the already approved agent.<sup>27</sup> <sup>90</sup>Y is produced commercially in a <sup>90</sup>Sr/<sup>90</sup>Y generator system where the <sup>90</sup>Sr is adsorbed on a solid support and <sup>90</sup>Y can be eluted in high specific activities.<sup>35</sup>

The well-established coordination chemistry of Y(III) was discussed earlier for <sup>86</sup>Y.

**Lutetium-177 ( $\beta^-$ ).** <sup>177</sup>Lu ( $t_{1/2}$  = 6.6 days) decays *via* the emission of three low energy  $\beta^-$  emissions with energies of 176 (12%), 384 (9%), and 497 keV (79%) used for radiotherapy.<sup>36</sup> In addition <sup>177</sup>Lu also emits two  $\gamma$  rays with maximum energies of 208 (11%) and 113 (6.6%) keV that can be used for SPECT imaging and dosimetry calculations.<sup>35,36</sup> <sup>177</sup>Lu has a long enough half-life that is best suited with biomolecules of long biological half-lives and the nuclide can be distributed to hospitals in remote regions. The low  $\beta^-$  energy emission is favourable for treating small metastases whilst minimizing kidney doses.<sup>36</sup> Despite its relatively long half-life, the radionuclide is part of one clinical trial in late phase II



investigating the therapeutic potential of a  $^{177}\text{Lu}$ -labelled peptide ( $^{177}\text{Lu}$ -DOTA-octreotate) for treatment of neuroendocrine tumours.<sup>27</sup>  $^{177}\text{Lu}$  is most commonly produced in a medium flux reactor *via* irradiation of enriched  $^{176}\text{Lu}$  (*via* the  $^{176}\text{Lu}(\text{n},\gamma)^{177}\text{Lu}$  reaction); this method gives  $^{177}\text{Lu}$  in high yields with medium to high specific activities at low cost.<sup>35,36</sup>

Lutetium is last in the lanthanide group and has the smallest atomic radius (86–103 pm for CN 6–9 respectively<sup>29</sup>), its most common oxidation state is +3 and Lu(III) commonly forms complexes of coordination number 9.<sup>36</sup>

**Rhenium-186/188 ( $\beta^-$ ).**  $^{188}\text{Re}$  ( $t_{1/2} = 17.0$  h) is a high energy  $\beta^-$  emitter (100%,  $E_{\text{max}} = 2.1$  MeV) that has many accompanying  $\gamma$ -ray emissions from the depopulation of excited daughter states and the 155 keV  $\gamma$  can be used for imaging.<sup>37,38</sup>  $^{186}\text{Re}$  ( $t_{1/2} = 3.7$  d) is a moderate energy  $\beta^-$  emitter ( $E_{\text{max}} = 1.02$  MeV, 91%) with an accompanying 137 keV  $\gamma$ -ray that can be used for imaging.<sup>35</sup>  $^{188}\text{Re}$  can be obtained from a  $^{188}\text{W}/^{188}\text{Re}$  generator, similar in design to the commonly used  $^{99\text{m}}\text{Tc}$  generator;  $\text{Na}^{188}\text{Re}(\text{V})\text{O}_4$  can be eluted from the generator in high specific activity with saline. The half-life of the parent  $^{188}\text{W}$  ( $t_{1/2} = 60$  d) permits the generator to be used for 2–6 months.<sup>35,37</sup> The production of  $^{186}\text{Re}$  is reactor-based *via* irradiation of  $^{185}\text{Re}$  with neutrons ( $^{185}\text{Re}(\text{n},\gamma)^{186}\text{Re}$ ) yielding low to medium specific activity  $^{186}\text{Re}$ .<sup>35,37</sup> Of the two isotopes,  $^{188}\text{Re}$  has garnered the most attention and is part of a completed Phase I trial for treatment of lung carcinomas, and a Phase I trial in recruiting stage for treatment of hepatocellular carcinomas.<sup>27</sup>

Rhenium, a group 7 transition metal, is a congener of Technetium. As a consequence Re shares parallel chemistry and isostructural complexes with Tc, and much of the same coordination chemistry employed in Tc radiopharmaceuticals can be adapted for Re. Although it is worth noting that  $[\text{ReO}_4]^-$ , the starting eluent from  $^{188}\text{Re}$  production, is harder to reduce than the  $^{99\text{m}}\text{Tc}$  analogue,  $[\text{TcO}_4]^-$ .<sup>37</sup> Rhenium exists in a range of oxidation states from +7 to –1, with an ionic radius of 53–63 pm (CN 6) for the +7 to +4 ions.<sup>29</sup> Much of the progress of Re(I) and Tc(I) radiopharmaceuticals has focused around the  $[\text{M}(\text{I})(\text{CO})_3]$  core. This *fac*- $[\text{M}(\text{CO})_3(\text{H}_2\text{O})_3]^+$  ‘tricarbonyl core’ has been thoroughly discussed and reviewed elsewhere.<sup>37,39</sup>

**Actinium-225 ( $\alpha$ ).**  $^{225}\text{Ac}$  has a 10 day half-life and can be incorporated into a radiopharmaceutical for  $\alpha$  therapy.  $^{225}\text{Ac}$  has been proposed to be used as an *in vivo* generator of its daughter isotope  $^{213}\text{Bi}$ , also an  $\alpha$ -emitter. This method has been developed by the Memorial Sloan-Kettering Cancer Center.<sup>40</sup> The decay of a single  $^{225}\text{Ac}$  ( $\sim 6$  MeV  $\alpha$  particle) goes predominantly through 6 daughters until it cascades to stable  $^{209}\text{Bi}$  producing in total 4  $\alpha$  and 3  $\beta^-$  emissions, and 2 useful  $\gamma$  emissions, the  $^{213}\text{Bi}$  440 keV  $\gamma$  emission can be used for imaging and dosimetry studies. Some of the intermediate daughters in the decay include  $^{221}\text{Fr}$  ( $t_{1/2} = 4.8$  min),  $^{217}\text{At}$  ( $t_{1/2} = 32.3$  ms), and  $^{213}\text{Bi}$  ( $t_{1/2} = 45.6$  min), each of which emits an  $\alpha$  particle.<sup>41</sup>  $^{225}\text{Ac}$  can be produced by natural decay of  $^{223}\text{U}$ , or by accelerator-based methods.<sup>41</sup> Actinium-225 has been incorporated primarily into antibody-based agents, two of which ( $^{225}\text{Ac}$ -Lintuzumab, and  $^{225}\text{Ac}$ -humanized anti-CD33 mAb (HuM195)) are currently in clinical trials.<sup>27</sup>

There are no stable isotopes of actinium, as a result the chemistry of actinium is virtually unknown; however, the

longer lived isotope  $^{227}\text{Ac}$  ( $t_{1/2} = 21.8$  years) could potentially be used to help elucidate the chemistry of actinium. The use of actinium in radiopharmaceuticals has a history of unfavourable radiolabelling chemistry and poor metal-chelate stability,<sup>42</sup> and the lack of an appropriate chelator that can stably bind the nuclide as well as control the fate of the daughters remains a challenge. Actinium isotopes in radiopharmaceuticals are typically +3 ions with a documented ionic radius of 112 pm (CN 3).<sup>29</sup> The large size is likely suited to large polydentate macrocyclic chelators of high denticity, since most commonly used chelates for Ac(III) (*vide infra*) range between 8–12 coordinate.<sup>41,43</sup>

**Bismuth-213 ( $\alpha$ ).** Bismuth-213 is an  $\alpha$  emitter with a half-life of 45.6 min and decays through two different pathways: *via*  $\alpha$  emission (2%, 5.8 MeV) followed by two  $\beta^-$  emissions, or  $\beta^-$  emission (98%) followed by an  $\alpha$  emission (8.4 MeV) and subsequent  $\beta^-$  emission to stable  $^{209}\text{Bi}$ .<sup>40</sup> In addition, a 440 KeV (26%) photon emission can be used for dosimetry studies.  $^{213}\text{Bi}$  can be generator produced from the decay of  $^{225}\text{Ac}$  in the  $^{225}\text{Ac}/^{213}\text{Bi}$  generator.<sup>44</sup> A clinically-used generator has been developed that can supply  $^{213}\text{Bi}$  for 10–15 days.<sup>40</sup> Despite its relatively short half-life, a  $^{213}\text{Bi}$ -labelled antibody agent ( $^{213}\text{Bi}$ -HuM195 (humanized anti-CD33)) was part of a clinical trial investigating the use of this agent in combination therapy with chemotherapy and has since completed.<sup>27,45</sup>

Bismuth is typically found in its +3 oxidation, with an ionic radius of 96–117 pm (CN 5–8).<sup>29</sup> Bi(III) has high affinity for oxygen and nitrogen donors, and also forms stable complexes with sulfur and halogens (especially iodide).<sup>46</sup> The large multidentate ligand CHX-A'-DTPA ( $\text{N}_3\text{O}_5$ ) (*vide infra*) has been used in many of the labelling studies of  $^{213}\text{Bi}$ -antibody conjugates,<sup>40,44</sup> and forms a dianionic octadentate complex with Bi(III).<sup>47</sup>

**Lead-212 ( $\alpha$  source).**  $^{212}\text{Pb}$  ( $t_{1/2} = 10.6$  hours) is a  $\beta^-$  emitter (100%, 570 keV) widely studied for  $\alpha$ -particle therapy, because it is the immediate parent radionuclide of the  $\alpha$ -emitter  $^{212}\text{Bi}$  ( $t_{1/2} = 60.6$  min).  $^{212}\text{Pb}$ -labelled mAbs can thus act as *in vivo* generators of  $^{212}\text{Bi}$ , extending the short half-life of  $^{212}\text{Bi}$ .<sup>48</sup> The bioconjugate  $^{212}\text{Pb}$ -TCMC-trastuzumab is in Phase I clinical trials for treatment of cancers that express the HER-2 antibody receptor.<sup>27</sup> The readily obtained  $^{224}\text{Ra}/^{212}\text{Pb}$  generator can be used for on-site production of either  $^{212}\text{Pb}$  or  $^{212}\text{Bi}$ , each can be specifically eluted by controlling the acid strength of the eluent. Due to the short half-life of  $^{224}\text{Ra}$  ( $t_{1/2} = 3.7$  d), the generator must be regenerated after 1–2 weeks.<sup>48</sup>

Lead is a post-transition metal with ionic radius of 119–149 ppm (2 + ion, CN 6–12).<sup>29</sup> Radionuclides of lead are found in their +2 oxidation state, classified as a borderline acid according to Pearson's hard-soft acid-base theory. The most common chelator of Pb(II) for radiopharmaceuticals, TCMC (*vide infra*), employs an octadentate ligand set with nitrogen and oxygen donor atoms.<sup>49</sup>

**Auger electron emitters.** Based on the LET and effective range of this radiation, Auger electron emissions are only effective as therapeutics if they can be internalized in the cell nucleus; this remains a great challenge. There are currently no FDA-approved agents or on-going clinical trials of radio-therapeutic Auger electron emitters.  $^{111}\text{In}$ , a popular SPECT radionuclide, also has an Auger electron emission (6.75 keV)

that has been used for therapy studies in one clinical trial of a radiolabelled tumour targeting peptide (Octreoscan,  $^{111}\text{In}$ -DTPA-D-Phe-octreotide).<sup>27,36</sup> Other Auger electron emitters such as  $^{201}\text{Tl}$  ( $t_{1/2} = 3.04$  days, 15.27 keV),  $^{203}\text{Pb}$  ( $t_{1/2} = 2.16$  days, 11.63 keV), and  $^{67}\text{Ga}$  ( $t_{1/2} = 3.26$  days, 6.26 keV),<sup>17</sup> better known for their accompanying imaging decays used in SPECT, have also recently gained some attention as potential Auger electron therapeutic nuclides,<sup>17,18</sup> but will not be a focus of this article.

## Bifunctional chelates (BFCs)

It is of utmost importance that the correct chelator matches a specific radiometal. Important properties of the metal–chelate complex as they relate to radiopharmaceutical design, such as thermodynamic stability, kinetic inertness, and complexation kinetics, must be evaluated (*vide supra*). The overall charge of the metal–chelate complex should also be taken into consideration since it may influence the biodistribution of the radiopharmaceutical. This is of less concern for bioconjugates of large molecular weight (e.g. monoclonal antibodies); however, for radiopharmaceuticals conjugated to peptides, small molecules, or antibody fragments, the metal–chelate complex plays a significant role in the overall pharmacokinetic behaviour of the system due to its relative size when compared to the targeting vector.

Common chelates utilised in radiopharmaceuticals can be grouped into two classes: acyclic (open chain) or macrocyclic (closed chain). Generally, acyclic chelates are less kinetically inert than macrocyclic complexes, even when thermodynamic stability ( $K_{\text{ML}}$ ) is comparable;<sup>8,24</sup> however, recent reports in the literature show good examples of acyclic chelators that exhibit both high thermodynamic stability with a specific metal and excellent kinetic inertness *in vitro*.<sup>52,53</sup> Acyclic chelators typically have faster metal-binding kinetics compared to macrocyclic analogues, a significant advantage for shorter-lived isotopes.

Despite the unique coordination chemistries of each metal, a few common chelators are used universally across a wide range of radiometals. Most notably, the tri- and tetraaza-based amino carboxylate macrocyclic chelators NOTA ( $\text{N}_3\text{O}_3$ ) and DOTA ( $\text{N}_4\text{O}_4$ ) and acyclic chelator DTPA ( $\text{N}_3\text{O}_5$ ) have been often used in radiolabelling experiments with many of the metals discussed herein despite less than optimal properties with many metals. Their prevalence in radiochemistry may stem from convenience rather than ‘best fit’ for a metal because their bifunctional analogues are commercially available. Recently, the trend is leaning towards metal-specific chelators that exhibit fast radiochemical labelling, high thermodynamic stability, and kinetic inertness in hopes to improve tumour-to-background ratios by eliminating radionuclide loss *in vivo*. Below, brief discussions of the most common chelators used in radiopharmaceutical applications are presented (Tables 5 and 6) with some new emerging examples.

### Acyclic chelators

EDTA ( $\text{N}_2\text{O}_4$ ) (ethylenediaminetetraacetic acid) and DTPA ( $\text{N}_3\text{O}_5$ ) (diethylenetriaminepentaacetic acid) are the most commonly exploited acyclic chelates in radiopharmaceutical chemistry.

DTPA (Table 5) has been used extensively for labelling of a variety of radiometals such as Cu(II) (CN 6,  $\log K_{\text{ML}} = 21.4$ ),<sup>8</sup> Ga(III) (CN 6,  $\log K_{\text{ML}} = 25.5$ ),<sup>8</sup> In(III) (CN 7,  $\log K_{\text{ML}} = 29.5$ ),<sup>8</sup> Y(III) (CN 8,  $\log K_{\text{ML}} = 22.0$ ),<sup>8</sup> and Zr(IV) (CN 8,  $\log K_{\text{ML}} = 35.8$ ).<sup>8</sup> Its large binding sphere and hard oxygen donor set make it a good candidate for making stable metal–ligand complexes with larger hard acidic cations. DTPA has been successfully incorporated into three FDA-approved radiopharmaceuticals ( $^{111}\text{In}$  based agents Octreoscan<sup>TM</sup> and ProstaScint<sup>®</sup>, and  $^{90}\text{Y}$  agent Zevalin) and it is the chelate in the most prescribed Gd MRI agent Magnevist<sup>TM</sup>.<sup>3</sup> More recently, a modified DTPA chelate, CHX-A'-DTPA ( $\text{N}_3\text{O}_5$ ) (Table 5), has shown great promise for In(III), Y(III) and Bi(III) isotopes. CHX-A'-DTPA is a commercial product and has been used in several clinical trials of  $^{111}\text{In}$ ,  $^{90}\text{Y}$ , and  $^{213}\text{Bi}$ .<sup>27,46</sup> CHX-A'-DTPA incorporates a more rigid chiral cyclohexyl (CHX-A') fragment into the backbone of DTPA in order to pre-organize the geometry of the donor atoms in hopes of improving kinetic inertness of the resulting metal complex.

DFO ( $\text{O}_6$ ) (desferrioxamine) (Table 5) is an acyclic chelator well-known for its application in iron chelation therapy; it possesses three hydroxamate groups for chelating metals and a terminal primary amine that can be used for conjugation to biomolecules. Due to the similarities between high spin Fe(III) and Ga(III), DFO also forms gallium complexes of high thermodynamic stability and has proven useful for conjugation to peptides and small molecules.<sup>30</sup> One application of DFO lies in its ability to label Zr(IV); it is the most popular choice for zirconium radiochemistry.<sup>33</sup> Neither thermodynamic stability constants nor crystal structure with Zr(IV) have yet been reported, nonetheless DFO has the ability to bind zirconium isotopes efficiently and rapidly. Excellent *in vitro* stability of the proposed  $[\text{Zr}(\text{DFO})(\text{H}_2\text{O})_2]^+$  complex has been documented (with less than 2% demetallation after seven days in serum);<sup>33</sup> however, recent small animal PET studies with a  $^{89}\text{Zr}$ -DFO-antibody demonstrate instability *in vivo* evinced by elevated uptake of  $^{89}\text{Zr}$  in bone.<sup>54</sup>

$\text{H}_2\text{dedpa}$  ( $\text{N}_4\text{O}_2$ ) (1,2-bis[[6-(carboxy)pyridine-2-yl]methyl]-amino}-ethane) (Table 5) is a new addition to the class of acyclic chelates that binds Ga(III) with high thermodynamic stability ( $\log K_{\text{ML}} = 28.1$ ),<sup>53</sup> and labels gallium isotopes quantitatively in 10 minutes at room temperature.  $[\text{Ga}(\text{dedpa})]^+$  shows high kinetic inertness *in vitro*, and remains up to 97% intact for 2 hours when incubated with excess *apo*-transferrin.<sup>53</sup> More recently, an octadentate  $\text{H}_2\text{dedpa}$  analogue,  $\text{H}_4\text{octapa}$  ( $\text{N}_4\text{O}_4$ ) (*N,N'*-bis(6-carboxy-2-pyridylmethyl)-ethylenediamine-*N,N'*-diacetic acid), has been reported that forms kinetically inert complexes with In(III), and may be a valuable alternative to the acyclic chelator DTPA for use with  $^{111}\text{In}$ .<sup>52</sup>

### Macrocyclic chelators

The popular tri- and tetraaza-based amino carboxylate macrocyclic chelators NOTA (1,4,7-triazacyclononane-1,4,7-triacetic acid) and DOTA (1,4,7,10-tetraazacyclododecane-1,4,7,10-tetraacetic acid) (Table 6), together with their bifunctional derivatives, form a class of ‘gold standards’ that have been used extensively in the labelling of a variety of radiometals for imaging and therapy. NOTA and DOTA are in themselves BFCs, one of the

**Table 6** Selected macrocyclic chelators and their bifunctional analogues (coupling moiety highlighted in blue)

Chelate	Native donor set	Metal ions ( $\log K_{ML}$ )	Bifunctional analogues
<p>NOTA</p>	$N_3O_3$	Cu(II) (21.6) <sup>a</sup> Ga(III) (31.0) <sup>a</sup> In(III) (26.2) <sup>a</sup>	<p><i>p</i>-SCN-Bz-NOTA  <math>n = 1</math>: NODASA  <math>n = 2</math>: NODAGA            NOTA (NO<sub>2</sub>A)</p>
<p>DOTA</p>	$N_4O_4$	Cu(II) (22.3) <sup>a</sup> Ga(III) (21.3) <sup>a</sup> In(III) (23.9) <sup>a</sup> Y(III) (24.4) <sup>a</sup> Lu(III) (25.5) <sup>b</sup> Zr(IV) Ac(III)	<p><i>p</i>-SCN-Bz-DOTA  <math>n = 1</math>: DOTASA  <math>n = 2</math>: DOTAGA            DOTA (DO<sub>3</sub>A)</p>
<p>TCMC</p>	$N_4O_4$	Pb(II)	<p><i>p</i>-SCN-Bz-TCMC</p>
<p><i>p</i>-NO<sub>2</sub>-Bz-PCTA</p>	$N_4O_3$	Ga(III) Cu(II) (19.1) <sup>c</sup>	<p><i>p</i>-SCN-Bz-PCTA</p>
<p>R = CH<sub>2</sub>CH<sub>2</sub>COOH TRAP</p>	$N_3O_3$	Ga(III) (26.2) <sup>d</sup>	<p>TRAP  <math>R = \text{---CH}_2\text{CH}_2\text{COOH}</math></p>

Table 6 (continued)

Chelate	Native donor set	Metal ions (log $K_{ML}$ )	Bifunctional analogues
 TETA	$N_4O_4$	Cu(II) (21.9) <sup>a</sup> Ga(III) (19.7) <sup>a</sup> In(III) (21.9) <sup>a</sup> Y(III) (14.8) <sup>a</sup> Lu(III) (15.3) <sup>b</sup>	 <i>p</i> -SCN-Bz-TETA TETA
 CB-TE2A	$N_4O_2$	Cu(II) Ga(III) In(III)	 CB-TE2A <i>p</i> -SCN-Bz-CB-TE2A
 Sar's	$N_6$	Cu(II) Ga(III)	 AmBaSar R =  NH <sub>2</sub> R' =  Diamsar R = R' =  NH <sub>2</sub>  SarAr R =  NH <sub>2</sub> R' =  BaBaSar R = R' =
 HEHA	$N_6O_6$	Ac(III)	 <i>p</i> -SCN-Bz-HEHA

<sup>a</sup> Ref. 8. <sup>b</sup> Ref. 55. <sup>c</sup> Ref. 58. <sup>d</sup> Ref. 61.

pendant carboxylic acid arms can be used in a conjugation strategy to form a peptide bond with a biomolecule. This direct method alters the native binding sphere and donor-ability of the chelators. Alternatively, an extra carboxylic pendant arm is added (to form NODASA/NODAGA and DOTASA/DOTAGA) or a separate conjugation moiety (*p*-SCN-Bz) is incorporated at a position that will minimize the effect on the metal binding ability of the ligand (to form *p*-SCN-Bz-DOTA or *p*-SCN-Bz-NOTA) (Table 6).

NOTA ( $N_3O_3$ ) has the smaller binding pocket of the two; it is most commonly used for gallium(III) isotopes (log  $K_{ML}$  = 31.0)<sup>55</sup> and is gaining popularity for copper(II) isotopes

(log  $K_{ML}$  = 21.6)<sup>55</sup> where it forms hexadentate complexes with each.<sup>28,55</sup> The [Ga(NOTA)] complex is also extremely stable to acid dissociation, and remained unchanged by NMR after 60 days in 6 M  $HNO_3$ .<sup>56</sup> NOTA has become particularly attractive for  $Ga^{3+}$  because of its ability to label gallium isotopes nearly quantitatively at room temperature and the high *in vivo* stability of the resulting complex.

DOTA ( $N_4O_4$ ) and its derivatives play an important role in clinical applications as it forms stable complexes with a variety of trivalent radiometals, such as  $^{68}Ga$  (log  $K_{ML}$  = 21.3),<sup>8</sup>  $^{86/90}Y$  (log  $K_{ML}$  = 24.3),<sup>8</sup>  $^{111}In$  (log  $K_{ML}$  = 23.9),<sup>8</sup>  $^{177}Lu$  (log  $K_{ML}$  = 25.5),<sup>55</sup>



and divalent nuclide  $^{64}\text{Cu}$  ( $\log K_{\text{ML}} = 22.3$ ).<sup>55,57</sup> Cu-DOTA conjugates are only moderately stable *in vivo* and demetallate, evinced by high liver accumulation of free copper.<sup>28,30</sup> DOTA has also been used extensively for labelling gallium isotopes, despite its less than optimal stability and need for heating to label quantitatively. Also, a variety of DOTA derivatives have been tested as BFCs for  $^{225}\text{Ac}$  with some success.<sup>42</sup>

Furthermore, an *N,N,N,N*-tetraamide analogue of DOTA, TCMC ( $\text{N}_4\text{O}_4$ ) (1,4,7,10-tetraaza-1,4,7,10-tetra-(2-carbamoyl methyl)-cyclododecane), displays favourable stability *in vitro* and *in vivo* with Pb(II) isotopes compared to DOTA,<sup>48,49</sup> and is the chelate of choice in a  $^{212}\text{Pb}$  clinical trial.<sup>27</sup> TCMC fully encapsulates the Pb(II), forming an octadentate complex with 4 nitrogen, and 4 amide oxygen donors.

The 12-membered tetraaza macrocycle, *p*-NO<sub>2</sub>-Bz-PCTA ( $\text{N}_4\text{O}_3$ ) (PCTA = 3,6,9,15-tetraazabicyclo[9.3.1]pentadeca-1(15), 11,13-triene-3,6,9-triacetic acid) (Table 6) exhibits favourable labelling and stability properties for copper ( $\log K_{\text{ML}} = 19.1$ )<sup>58</sup> and gallium isotopes.<sup>30</sup> The chelate incorporates a *p*-nitrobenzyl moiety that can be converted into an isothiocyanate for attachment of targeting groups. *p*-NO<sub>2</sub>-Bz-PCTA exhibits much faster complex formation compared to DOTA for gallium with the ability to rapidly and efficiently label  $^{68}\text{Ga}$  (>96% RCY) at room temperature in 10 minutes, and exhibits high kinetic inertness *in vitro* when incubated with apo-transferrin (less than 10% transchelated with transferrin after 4 hours).<sup>59</sup> *In vivo*, the biodistribution of  $^{68}\text{Ga}$ -labelled *p*-NO<sub>2</sub>-Bn-PCTA is similar to that of the analogous *p*-NO<sub>2</sub>-Bz-DOTA complex, circulating in the blood and excreted through the kidneys over 4 hours, suggesting *p*-NO<sub>2</sub>-Bz-PCTA may be an improved alternative to DOTA in Ga based radiopharmaceutical development.<sup>59</sup> The chelate can also rapidly and efficiently label  $^{64}\text{Cu}$  (>98% RCY) in 5 minutes at room temperature.<sup>60</sup>

TRAP (previously known as PrP9) ( $\text{N}_3\text{O}_3$ ) (1,4,7-triazacyclononane-1,4,7-tris[methyl(2-carboxyethyl)phosphinic acid]) (Table 6) is a new addition to the family of macrocyclic chelators for gallium; it is derived from a NOTA-type framework with phosphinic acid arms replacing the carboxylic acid arms. TRAP shares strong thermodynamic stability with Ga(III) ( $\log K_{\text{ML}} = 26.2$ ),<sup>61</sup> and has the ability to incorporate  $^{68}\text{Ga}$  nearly quantitatively (>95% RCY) at low concentrations in even strongly acidic media in 5 minutes at 60 °C.<sup>61,62</sup> In addition, the three carboxylic pendant arms attached to the phosphinic acids provide a convenient way for introduction of three targeting groups through a peptide bond conjugation strategy.

The tetraazamacrocyclic TETA ( $\text{N}_4\text{O}_4$ ) (1,4,8,11-tetraazacyclotetradecane-1,4,8,11-tetraacetic acid) (Table 6) has been extensively used for Cu(II) radiopharmaceuticals. Cu(II) shares a similar thermodynamic stability with TETA and DOTA ( $\log K_{\text{ML}} = 21.9$  and 22.3, respectively)<sup>8</sup> although  $[\text{Cu}(\text{TETA})]^{2-}$  complexes are more kinetically inert compared to  $[\text{Cu}(\text{DOTA})]^{2-}$ , but still suffer from radiocopper loss *in vivo*.<sup>63,64</sup>

To improve on the stability of the TETA framework, the cross-bridged analogue CB-TE2A ( $\text{N}_4\text{O}_2$ ) (1,4,8,11-tetraazabicyclo[6.6.2]-hexadecane-4,11-diyl)diacetic acid) (Table 6) exhibits greatly improved stability of copper complexes; however, labelling CB-TE2A with Cu(II) isotopes requires rigorous heating (>90 °C)

and prolonged reaction times (~1 h), which impedes its use with thermally sensitive biomolecules.<sup>28,30</sup>

The sarcophagine type bifunctional chelators ( $\text{N}_6$ ) (sarcophagine = Sar = 3,6,10,13,16,19-hexaazabicyclo[6.6.6]icosane) (Table 6) are the most recent addition to the class of ligands employed for radiocopper labelling, but have also been evaluated for  $^{68}\text{Ga}$ .<sup>30</sup> Sarcophagines have the ability to label micromolar concentrations of  $^{64}\text{Cu}$  quantitatively at room temperature in minutes.<sup>28</sup> In addition, the  $[\text{Cu}(\text{Sar})]$  complexes exhibit high *in vitro* kinetic inertness against mouse serum (>98% intact after 4 hours).<sup>65</sup> These characteristics make Sar cages a promising scaffold for incorporation into copper-radiopharmaceuticals of thermally sensitive biomolecules.<sup>28,30</sup> Labelling with  $^{68}\text{Ga}$ , however, requires heating at 85 °C for 30 min.<sup>30</sup>

The large 12-coordinate ( $\text{N}_6\text{O}_6$ ) ligand HEHA (1,4,7,10,13,16-hexaazacyclohexadecane-1,4,7,10,13,16-hexaacetic acid) (Table 6) has been investigated primarily for radiolabelling of the large radiometal  $^{225}\text{Ac}$ , and has been successfully conjugated with a variety of antibodies.<sup>43</sup> Radiolabelling with  $^{225}\text{Ac}$  at 37 °C, yields RCYs of 60–85% after 30 minutes. The bioconjugates exhibited adequate stability in bovine serum at 37 °C during early time points; however, later time points suggest more than one-third of the  $^{225}\text{Ac}$ -HEHA-bioconjugate degraded or transchelated with serum proteins.<sup>43,66</sup>

## Linker-bioconjugation strategies

The placement and mode of attachment of the BFC to the biomolecule is important; it is crucial that this conjugation does not interfere with the binding ability of the chelate to metal ion, or the affinity of the biomolecule for its intended target. Often the targeting vectors are sensitive biomolecules which risk degradation when heated, so it is best if the conjugation strategy occurs rapidly at mild temperatures to retain the integrity of the targeting vector. Predominantly, four conjugation strategies are employed extensively in radiopharmaceutical construction: peptide, thiourea, thioether, and click chemistry triazole bonds (Fig. 4). Often biomolecules have primary amines or free thiols in their structure for conjugation to a BFC, so all that remains is to introduce a conjugation moiety on the chelate that is compatible with the functional group(s) on the biomolecule.

Peptide bond formation involves coupling of a carboxylic acid to a primary amine with the aid of a coupling agent such as HATU (*O*-(7-azabenzotriazol-1-yl)-*N,N,N',N'*-tetramethyluronium hexafluorophosphate), HOBt (hydroxybenzotriazole) or EDC (1-ethyl-3-(3-dimethylaminopropyl)carbodiimide), or a carboxylic acid activated with a succinimidyl (NHS) ester is coupled to a primary amine without the need for additional coupling agents.<sup>13</sup> Many of the chelators used in radiochemistry have several carboxylic arms, and selective peptide formation with one of the arms can be accomplished by controlling the mole ratios of chelate to targeting vector, and/or using protecting group chemistry to shield the other carboxylic acid pendant arms from conjugating with the primary amine on the biomolecule. Peptide bond formation is among the most popular conjugation strategy used in peptide-bioconjugates; the peptide coupling reaction is



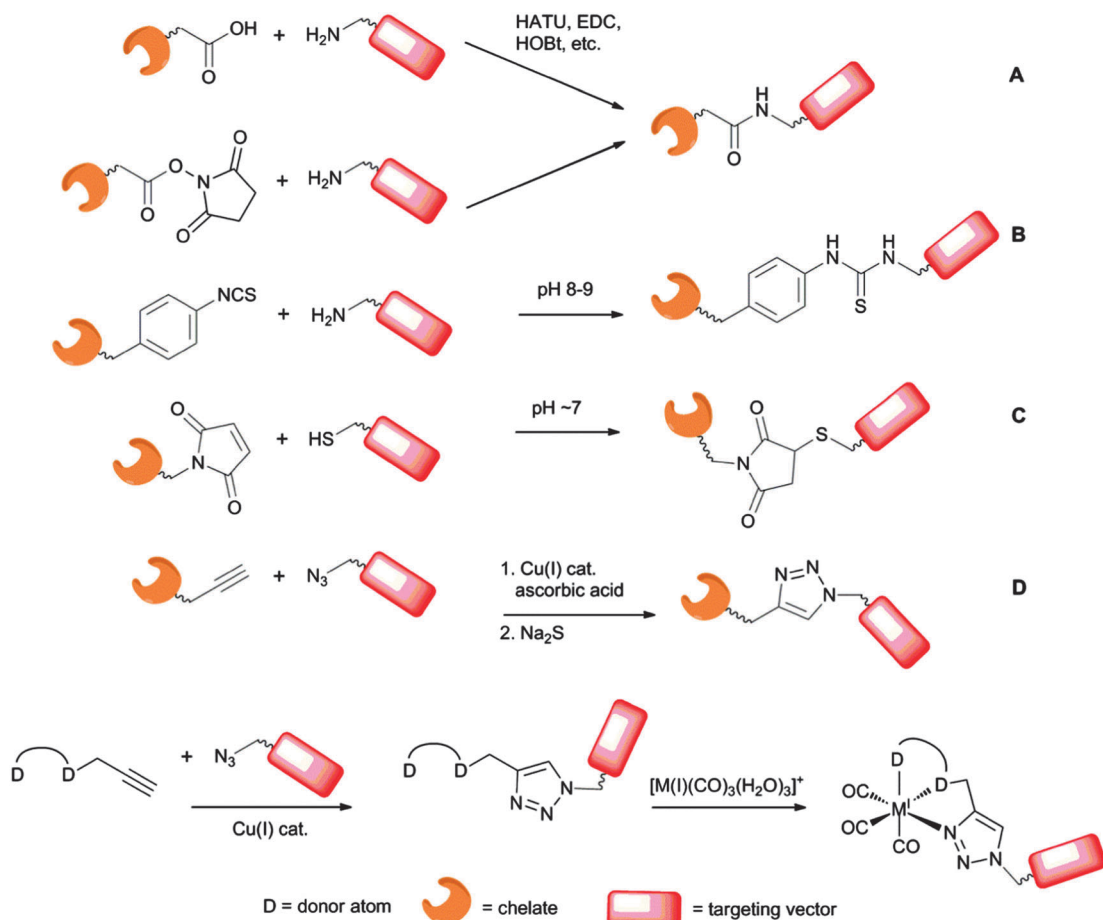


**Fig. 4** Four common types of bioconjugation bond forming reactions: (A) peptide; (B) thiourea; (C) thioether; and (D) triazole-click. (E) "Click-to-chelate" method for  $M(I) = Re(I)/Tc(I)$ .

often done on a solid peptide resin followed by full deprotection of the chelate and cleavage from the resin.

Thioether bond formation links a thiol with a maleimide and occurs under mild conditions (pH 7.2 to 7.4) without the need for heating or catalyst. This reaction has been used for coupling of both peptides and proteins, where thiol groups are naturally present and used for conjugation to a BFC that has been functionalized with a maleimide.<sup>67</sup> Thiourea bond formation couples an isothiocyanate to a primary amine; this reaction must be done in slightly basic conditions (pH 8–9) where the deprotonated amine is required for reactivity.<sup>67</sup> Generally, thiourea bond formation is slower than thioether coupling,<sup>67</sup> but both reactions can be accomplished on the fully deprotected ligand.

The copper-catalyzed 1,3-dipolar Huisgen cycloaddition occurs between terminal alkynes and azides to form a 1,4-substituted triazole, and is often termed the "click" reaction.<sup>67</sup> Use of a Cu(I) catalyst leads to fast reaction times, and controls the regioselectivity of the reaction. Furthermore, both functional groups (azide and alkyne) are stable to most common coupling conditions and can be introduced into the chelate or biomolecule with relative ease.<sup>67</sup> Although a copper catalyst in a reaction involving a chelate can lead to copper complexation, copper is readily removed by quenching the reaction with Na<sub>2</sub>S

to precipitate the cupric sulfide. The resulting triazole carries electron-rich nitrogen atoms, which in some cases can act as additional donor atom(s) to the metal ion.<sup>68,69</sup> This method, dubbed "click-to-chelate", was first developed for the attractive *fac*-[M(I)(CO)<sub>3</sub>(L)<sub>3</sub>]<sup>+</sup> tricarbonyl core ( $M(I) = Re/Tc(I)$ ) and has recently been extended for use with other radiometals.<sup>68,69</sup> It can provide an elegant method for adding the necessary donor atoms for the metal through the N3 of the 1,2,3-triazole ring while simultaneously incorporating the targeting vector (Fig. 4).<sup>70</sup>

## Targeting vectors

The physiological traits of cancer suit the use of radiopharmaceuticals for the specific detection and treatment of the complex disease. When a cell becomes cancerous a cascade of biochemical responses occurs, and as a result the diseased cells exhibit many biomarkers that, although present in normal cells, are either mutated or over-expressed.<sup>57,71,72</sup> Various surface receptors are over-expressed in particular tumour types, and radiolabelled biomolecules that bind to these receptors can be used to visualize tumours scintigraphically, or deliver a therapeutic radiation dose to them specifically (Fig. 5). There has been tremendous progress in the identification of these over-expressed surface receptors

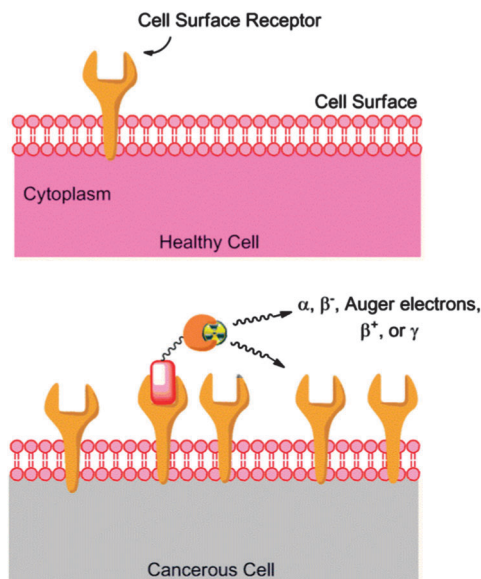


**Fig. 5** Targeting over-expressed cell surface receptors in cancerous tissue with radiopharmaceuticals.

(antigens) and the native ligands (biomolecules) that bind to them.<sup>55,73</sup> The choice of targeting vector is crucially important in the development of a successful radiopharmaceutical, since the effectiveness of targeted therapies depends on the molecular target expression in the patient. The antigen must be sufficiently over-expressed compared to neighbouring healthy tissue so as to create a positive response, and the biomolecule must bind specifically with high affinity to the desired antigen.<sup>15,66</sup>

There are also passive ways to target cancer cells based on such unique characteristics as the enhanced vascular permeability of tumour blood vessels, and poor lymphatic drainage systems, known collectively as the enhanced permeability and retention (EPR) effect, or tumour microenvironment such as reduced pH or reduced oxygen concentration.<sup>74</sup> Herein we will focus on the use of biomolecules (antibodies, peptides, and antibody fragments) that target over-expressed receptors on the surface of cancer cells.

### Biomolecules

Many biomolecules have been used to target surface receptors on cancer cells. Most commonly peptides, antibodies, antibody fragments, small molecules,<sup>72</sup> and more recently, nanoparticles<sup>75</sup> have been conjugated to a BFC. Each class of biomolecules has different biological properties, such as varying biological half-lives, and these properties must be matched with the physical properties of the radionuclide. In general, molecular size greatly influences circulation time; the larger the molecule the longer it will take to accumulate in tumours. In order to produce a clear image or minimize radiation dose to healthy tissue, the radiopharmaceutical should specifically accumulate at high levels within the tumour target sites and unbound agent should clear from the blood within a time frame compatible with the radioactive half-life of the nuclide.<sup>15</sup> A few of the most popular targeting vectors of choice for radiopharmaceuticals are discussed below, highlighting their

strengths and weaknesses, as well as important factors affecting their potential for use in radiopharmaceuticals.

### Antibodies

An antibody (Ab), also known as an immunoglobulin (Ig), is a large Y-shaped protein of relatively high molecular weight (140–160 kDa).<sup>72</sup> Upon their discovery, monoclonal antibodies (mAbs) were termed “magic bullets” because they were thought to be widely applicable in cancer therapy; however, their use to date remains limited due to reduced accumulation in tumours and relatively slow blood clearance (3–4 weeks) resulting in only moderate tumour-to-background ratios.<sup>15</sup> Nonetheless, there are four FDA-approved radiolabelled mAbs on the market, Bexxar (<sup>131</sup>I agent), Zevalin (<sup>90</sup>Y-labelled ibritumomab tiuxetan), ProstaScinta® (<sup>111</sup>In agent), and a <sup>99m</sup>Tc agent,<sup>3</sup> in addition there are dozens of clinical trials currently testing the efficacy of radiolabelled antibodies.<sup>27</sup> Because of their long biological half-lives *in vivo*, the antibody must be matched with a radioisotope that has a comparably long half-life, in order to allow for tumour accumulation and non-specific clearance. <sup>89</sup>Zr ( $t_{1/2}$  = 3.3 days) has been suggested as a good suitor for immunoPET, and much effort is being made towards a <sup>89</sup>Zr-immuno-conjugate.<sup>76</sup>

Another consequence of their large size, mAbs have multiple functional groups available on their surface making it difficult to control the number and location of BFC attachments in conjugation reactions; often multiple chelates can be attached to a single antibody. The number of chelates attached per antibody can be deduced through an isotopic dilution method and is controlled by altering the BFC to antibody molar ratios.<sup>13</sup> It is usually favourable to introduce as much radioactive-binding capability as possible without negatively affecting the binding affinity of the antibody to its antigen.

### Peptides

Peptides have a broad range of biological targets and have desirable pharmacokinetic characteristics, such as high uptake in target tissue and rapid clearance from blood and non-target tissue, that are favourable for incorporation into a radiopharmaceutical. Moreover, peptides can be easily chemically modified and radiolabelled in many ways, and have garnered much interest as targeting vectors for radiopharmaceutical purposes. FDA-approved Octreoscan™ (<sup>111</sup>In-DTPA-octreotide) is one example of a radiolabelled peptide used in SPECT imaging.<sup>3</sup> The fast localization and clearance of peptides suggests they are well suited to radioisotopes of short half-life; in this respect much effort is being made towards peptide bioconjugates of <sup>68</sup>Ga ( $t_{1/2}$  = 68 min) with several clinical trials in progress.<sup>27</sup>

Most naturally occurring peptides are prone to rapid enzymatic degradation; in order to improve their metabolic stability, peptides have been engineered that incorporate non-natural amino acids residues, amino alcohols, or cyclic peptides, these modifications must not affect the native binding affinity of the peptide for the antigen.<sup>55,77,78</sup> A spacer can also be introduced to the end of the peptide before it is conjugated to the BFC, in order to minimize or eliminate any interference between the two moieties, or act as a pharmacokinetic modifier.

Most commonly used spacers include short amino acid sequences (dimer or trimer of  $\beta$ -Ala, Gly, or  $N^{\epsilon}$ -amino hexanoic acid), low molecular weight polyethylene glycol (PEG), or hydrocarbon chains.<sup>77</sup> The length, flexibility, hydrophobicity and charge should be considered when selecting an appropriate spacer, as their introduction can greatly influence the biodistribution of the radiopharmaceutical.<sup>77</sup>

Solid-phase peptide synthesis (SPPS) is widely used and can easily prepare peptides with a variety of modifications.<sup>79</sup> The appropriate binding site can be introduced on the end of the peptide, and the point of conjugation to BFC can be controlled, and is typically set at 1 : 1 chelate to peptide.

### Other biomolecules and targeting vectors

Other biomolecules being investigated as targeting moieties in radiopharmaceuticals include antibody fragments, oligonucleotides,<sup>80</sup> and nanoparticles.<sup>74,75</sup> With the addition of these biomolecules, there is a large library of targeting vectors with varying pharmacokinetic properties to choose from.

Advances in protein engineering have led to a range of antibody fragments of varying sizes with corresponding varying pharmacokinetic properties that can be used as targeting vectors in radiopharmaceutical design. Examples of antibody fragments include scFv (single-chain variable fragment, 25 kDa), diabodies (50 kDa), Fab (fragment, antigen binding, 55 kDa), minibodies (80 kDa), and F(ab')<sub>2</sub> (110 kDa), each is comprised of different domains of an intact mAb and nevertheless retain the specificity and affinity of the parental antibody.<sup>81,82</sup> Affibodies are the newest type of antibody fragment that have been exploited as an antibody mimetic; they are engineered molecules of 58 amino acid residues (6–7 kDa) with a three- $\alpha$ -helical bundle structure derived from one of the binding domains of a fully intact antibody. In general, biological half-life of antibody fragments is inversely proportional to the molecular weight of the molecule. With their reduced size antibody fragments exhibit faster blood clearance (<10 h for an Affibody compared to 3–4 weeks for the full mAb),<sup>83</sup> which means faster acquisition times for imaging purposes, and lower non-specific radiotoxicity for therapeutic isotopes. In turn, the isotopes used with antibody fragments can have shorter half-lives. For example, a <sup>68</sup>Ga-labelled antibody fragment, F(ab')<sub>2</sub>-trastuzumab, has shown great promise for PET imaging of solid tumours that express the HER-2/*neu* receptor,<sup>84</sup> and is currently in clinical trials.

The use of nanoparticles as targeting vectors in nuclear medicine does not rely on the ability of the particle to bind to an over expressed surface receptor; instead the biodistribution of nanoparticles is dominated by their large size and ability to take advantage of the EPR effect of cancer tissue (*vide supra*), where 'leaky' vessels of poorly vascularized tumours allow for the uptake and retention of large macromolecules. To improve the tumour-targeting ability of nanoparticles, traditional targeting vectors, such as peptides or antibodies, are often introduced onto their surface.<sup>85</sup>

### Biological targets

For an antigen to be selected as an appropriate target it must be readily accessible, highly overexpressed and preferably

expressed only within the desired target tissue.<sup>15</sup> In addition, some antigens internalize their binding ligands and as a consequence trap the radiopharmaceutical in the cell. This trait is attractive for radiotherapy, where complex and multi-daughter decay pathways of therapeutic nuclides complicate the stability of the metal–chelate complex. For Auger electron emitters that must reach the nucleus to cause cell death, internalization into the cytoplasm is the first step in entering the nucleus. An exhaustive review of all antigens that have been targeted with radiopharmaceuticals is beyond the breadth of this article, some comprehensive reviews outlining the peptide<sup>55,57,77,79,86–88</sup> and antibody<sup>15,50</sup> binding antigens can be found elsewhere. Instead some of the most popular antigens being investigated will be outlined and accompanied with a few specific examples highlighting the potential of radiometals in the field of imaging and treatment of cancers.

Common peptide binding antigens implicated on human cancers include the integrin, somatostatin (SST), Gastrin-releasing peptide (GRP), Melanocortin 1 (MC1), and cholecystokinin 2 (CCK2)/gastrin receptors. Frequently targeted antibody receptors include HER-2/*neu*, Epidermal Growth Factor (EGF), and Vascular Endothelial Growth Factor (VEGF) (Table 7). Many of these receptors are implicated on a variety of cancer types presenting a broader platform for their use in the clinic.<sup>50,77</sup>

In most cases the receptor's native targeting molecule is not an appropriate choice for use *in vivo* due to rapid degradation (of peptides) or slow blood circulation time (of mAbs); thus, analogues of native ligands have been fabricated which retain the binding avidity to the target antigen, while exhibiting favourable pharmacokinetic behaviour *in vivo*.

The naturally occurring cyclic neuropeptide somatostatin (SST) that binds the SST receptor with high affinity is rapidly degraded *in vivo* by enzymes, eliminating its potential for use *in vivo*. Analogues of the SST peptide, such as octreotide (OC) and octreotate (TATE) (Fig. 6), are stable to enzymatic degradation while maintaining high binding affinity and specificity for the SST receptor. <sup>68</sup>Ga-DOTA-TOC (<sup>68</sup>Ga-DOTA-Tyr<sup>3</sup>-octreotide) is a popular example of a radiolabelled peptide which targets the SST receptor; the success of this radiopharmaceutical has stimulated much of the development of <sup>68</sup>Ga radiopharmacy and the <sup>68</sup>Ge/<sup>68</sup>Ga generator.<sup>31,89</sup> Despite NOTA forming complexes with gallium of higher stability and faster radiolabelling chemistry than DOTA,<sup>89</sup> the latter was chosen as the BFC and generated promising biodistribution of the labelled bioconjugate. This example demonstrates the importance of finding a balance between metal–complex stability without compromising the biodistribution of the biovector.

Integrin receptors are a popular class of cell surface receptors that have been implicated in many human cancers and utilised as a target for tumour-targeting radiopharmaceuticals.<sup>8,55</sup> The  $\alpha_v\beta_3$  integrin receptor is the most popular, and has been extensively targeted with the cyclic peptide RGD (Arg-Gly-Asp)<sup>90</sup> (Fig. 6). A variety of radiolabelled-RGD bioconjugates have been investigated for their ability to selectively image or treat  $\alpha_v\beta_3$  integrin receptor-positive tumours using radiometals such as <sup>177</sup>Lu,<sup>91</sup> <sup>64</sup>Cu,<sup>92</sup> <sup>111</sup>In,<sup>93</sup> <sup>68</sup>Ga,<sup>94</sup> or <sup>90</sup>Y.<sup>95</sup>

**Table 7** Selected target antigens and their associated biomolecules with an example of use

Target antigen receptor	Biomolecule	Ligand type	Example	Ref.
$\alpha_v\beta_3$ Integrin	Arg-Gly-Asp (RGD)	Peptide	$^{177}\text{Lu}$ -DTPA-Glu-cyclo(RGDfK)	91
Somatostatin	Somatostatin (SST) Octreotide (OC)	Peptide	$^{213}\text{Bi}$ -DOTATOC (OC = octreotide)	103
Gastrin-releasing peptide (GRP)	Gastrin-releasing peptide (GRP) Bombesin (BBN)	Peptide	$^{64}\text{Cu}$ -Sar(NH <sub>2</sub> ) <sub>2</sub> -BBN <sub>2</sub> (BBN <sub>2</sub> = Lys <sup>3</sup> -Bombesin)	104
Melanoma <i>i.e.</i> Melanocortin 1 (MC1)	$\alpha$ -Melanocyte-stimulating hormone ( $\alpha$ -MSH)	Peptide	$^{111}\text{In}$ -DOTA-ReCCMSH (ReCCMSH = Re cyclized analogue of $\alpha$ -MSH)	105
Cholecystokinin 2 (CCK2)/gastrin	Cholecystokinin (CCK)	Peptide	$^{111}\text{In}$ -DOTA-sCCK8 (sCCK8 = peptide analogue of CCK)	106
HER-2/ <i>neu</i> (a.k.a erbb-2)	Trastuzumab (Herceptin)	Antibody	$^{89}\text{Zr}$ -DFO-trastuzumab	76
Epidermal growth factor (EGF)	Epidermal growth factor (EGF)	Antibody	$^{68}\text{Ga}$ -DOTA-hEGF (hEGF = 53 amino acid EGF peptide analogue)	107
Vascular endothelial growth factor (VEGF)	Bevacizumab (Avastin)	Antibody	$^{86}\text{Y}$ -CHX-A''-DTPA-bevacizumab	108

Recently, the targeting ability of a peptidomimetic ligand LLP2A, which targets the less explored  $\alpha_4\beta_1$  integrin receptor with high affinity, has been investigated.<sup>96</sup> The peptide was labelled with  $^{64}\text{Cu}$  using a second generation cross-bridged macrocycle CB-TE1A1P (a CB-TE2A derivative where one pendant arm has been replaced with a methane phosphinic acid pendant arm) and evaluated against the corresponding CB-TE2A-bioconjugate.<sup>30</sup> The chelate-bioconjugate CB-TE1A1P-LLP2A was prepared on a peptide resin and subsequently labelled with  $^{64}\text{Cu}$ . Quantitative labelling was achieved after 60 min at room temperature or after 5 min at 90 °C; a marked improvement from the first generation analogue CB-TE2A, well known for its sluggish labelling kinetics with copper isotopes requiring heating at 90 °C for 1 hour (68% RCY). Small animal model studies with  $^{64}\text{Cu}$ -CB-TE1A1P-LLP2A showed dramatically improved tumour-to-background contrast compared to the  $^{64}\text{Cu}$ -CB-TE2A analogue. This example highlights the advantages of exploring new BFCs with improved binding kinetics.

Another popular antigen targeted by radiolabelled peptides is the melanocortin-1 (MC-1) receptor, which is a promising melanoma-specific target that binds the linear tridecapeptide  $\alpha$ -melanocyte stimulating hormone ( $\alpha$ -MSH) with nanomolar affinity.<sup>57</sup> These receptors are over expressed on the surface of human malignant melanomas, which bind and internalize their ligands leading to their sequestration in the cytoplasm. Much like other native peptides,  $\alpha$ -MSH is degraded *in vivo* by enzymes, hence several synthetic candidate peptides have been tested as analogues<sup>57,97</sup> (Fig. 6). A report recently evaluated an  $\alpha$ -MSH analogue, Re(Arg<sup>11</sup>)CCMSH, labelled with  $^{111}\text{In}$ ,  $^{86}\text{Y}$ , and  $^{68}\text{Ga}$  in PET/SPECT imaging of melanoma;<sup>98</sup> this rhenium cyclized peptide analogue of  $\alpha$ -MSH has also been studied by other groups.<sup>99</sup> The melanoma targeting peptide-bioconjugate CHX-A''-DTPA-Re(Arg<sup>11</sup>)CCMSH was prepared on a solid-phase peptide resin.  $^{111}\text{In}$ -labelling was accomplished at 40 °C for 40 minutes,  $^{86}\text{Y}$ -labelling at 75 °C for 30 minutes, and  $^{68}\text{Ga}$ -labelling at 85 °C for 20 minutes, to obtain RCYs >95% and radiochemical purity >95% for all nuclides with little or no purification. All three agents were able to selectively target melanoma tumours, and clearly image the lesions. The biodistribution studies showed rapid tumour uptake after 2 hours, and excess radioactivity in non-target tissues was eliminated and excreted mainly through the kidneys.

The gastrin-releasing peptide receptor (GRPr), another popular peptide specific antigen found on a wide variety of human cancers such as lung, prostate, and breast cancer, exhibits high affinity for the 14 amino acid peptide bombesin (BBN).<sup>8</sup> Various modifications that increase metabolic stability, influence binding properties or biodistribution behaviour of the native bombesin peptide have been made (Fig. 6), and exploited in conjugation reactions to BFCs.<sup>57,100</sup> Recently, a new conjugate of bombesin, JMV594, as an antagonist for targeting the GRPr for SPECT imaging with  $^{111}\text{In}$  was explored.<sup>101</sup> In addition, a positively charged spacer (4-amino-1-carboxymethyl-piperidine) was attached between the BFC and peptide to act as a pharmacokinetic modifier. The DOTA-linker-JMV594 bioconjugate was prepared on a peptide resin and subsequently labelled with  $^{111}\text{In}$  at 95 °C for 30 min (RCY >95%). Biodistribution studies showed that  $^{111}\text{In}$ -DOTA-JMV594 was taken up quickly by the tumour and pancreas; however, uptake in the pancreas washed out over longer time points, while radioactivity remained in the tumour.<sup>101</sup> These results suggest  $^{111}\text{In}$ -DOTA-JMV594 may be a good candidate for testing in humans.

The HER-2/*neu* receptor is over expressed in 25–30% of human breast cancers<sup>8</sup> and is a popular target in radiopharmaceuticals; several radiometals ( $^{111}\text{In}$ ,  $^{64}\text{Cu}$ ,  $^{89}\text{Zr}$ , and  $^{212}\text{Pb}$ ) conjugated to the monoclonal antibody trastuzumab (sold under the trade name Herceptin), known to target the HER-2/*neu* receptor, or analogous antibody fragments ( $^{68}\text{Ga}$ ) can be found in clinical trials.<sup>27</sup> In a study by Costantini *et al.*, the effect of known radiosensitizing drugs (methotrexate, paclitaxel, and doxorubicin) on the effectiveness of the Auger emitter  $^{111}\text{In}$  was studied in a  $^{111}\text{In}$ -DTPA-NLS-trastuzumab bioconjugate.<sup>102</sup> The  $\gamma$  emission of  $^{111}\text{In}$  was used in dosimetry studies and SPECT imaging of the radiotherapeutic agent. The therapeutic effects of Auger electron emitters have been limited in the past due to poor localization in the cell nucleus, where the radioactivity is at an active range to cause cell death. Combination therapy with radiosensitizing drugs to amplify the lethal effects of ionising radiation has been proposed as a way to increase the therapeutic effectiveness of radiotherapy.  $^{111}\text{In}$ -DTPA-NLS-trastuzumab, is equipped with two targeting vectors; trastuzumab for specific targeting of the HER-2/*neu* receptor, and a synthetic 13 mer nuclear-localization sequence (NLS) which promotes



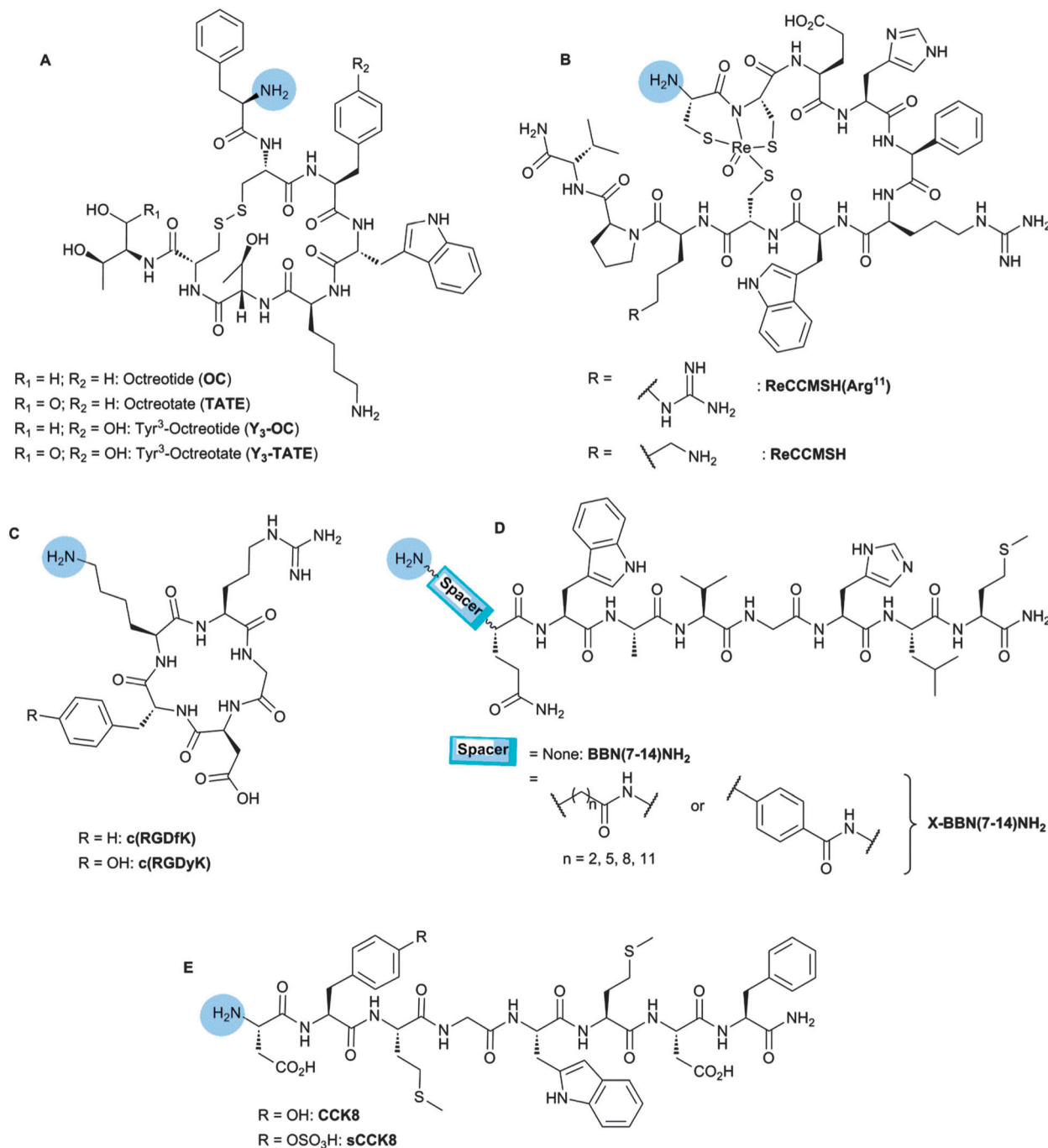


**Fig. 6** Selected targeting peptides for surface receptors: (A) somatostatin (SST), (B) melanocortin 1 (MC1), (C)  $\alpha_v\beta_3$  integrin, (D) gastrin-releasing peptide (GRP), and (E) cholecystinin 2(CCK2)/gastrin. Moiety used in conjugation reactions highlighted in blue.

nuclear importation after HER-2 mediated internalization into the cancer cell. Synthesis of the bioconjugate resulted in the chelate:mAb:NLS-peptide ratio of 15:1:60. <sup>111</sup>In-labelling was accomplished at room temperature for 60 minutes to achieve radiochemical purity >97% after filtration purification.<sup>102</sup> The study found the co-administration of the radiosensitizing drugs increases the efficacy of the targeted Auger electron radiotherapy of <sup>111</sup>In-DTPA-NLS-trastuzumab.<sup>102</sup>

Despite some success with radiolabelled monoclonal antibodies, most still suffer from poor tumour-to-background ratios and

sluggish blood clearance. To overcome these limitations, many research groups are investigating mAb fragments that can target these antibody specific receptors. The epidermal growth factor receptor (EGFR) is an attractive target antigen that is over expressed in a wide range of tumours including human breast cancer, and small cell carcinoma of the head and neck; it binds the primary ligands epidermal growth factor (EGF) and transforming growth factor- $\beta$  (TGF $\beta$ ), two mAbs.<sup>72</sup> A recent study implemented the anti-EGFR Affibody Z<sub>EGFR:1907</sub> in a <sup>177</sup>Lu-radiotherapeutic.<sup>83</sup> In previous studies radiolabelled-Z<sub>EGFR:1907</sub> showed



excellent targeting to EGFR-positive tumours, but persistent and high renal uptake. In an attempt to improve the pharmacokinetic properties, a second targeting vector was added (large protein human serum albumin (HSA)), to keep the radiopharmaceutical in blood circulation and away from the renal system. A DO3A-HSA-Z<sub>EGFR:1907</sub> bioconjugate was prepared with 1–5 Affibodies per HSA protein introduced. Labelling of <sup>177</sup>Lu was performed at 39 °C for 1 hour (>70% RCY) after purification. An *in vitro* stability assay of <sup>177</sup>Lu-DO3A-HSA-Z<sub>EGFR:1907</sub> against an excess of mouse serum resulted in >95% of the probe intact at 4 hours, and >80% intact at longer time points (24–168 h). Biodistribution studies showed long retention of the radiopharmaceutical in the tumour and good tumour contrast in SPECT images. <sup>177</sup>Lu-DO3A-HSA-Z<sub>EGFR:1907</sub> showed lower uptake in the kidneys compared to the <sup>177</sup>Lu-DO3A-Z<sub>EGFR:1907</sub> alone,<sup>83</sup> but instead high and persistent liver uptake was seen which may suggest the introduction of such a large protein has influenced the pharmacokinetic and metabolic behaviour of the radiopharmaceutical towards the liver.

These few examples represent a span of target antigens and biomolecules, nonetheless some broadly applicable conclusions can be drawn. Specifically, small changes in one system can lead to large impacts on the pharmacokinetic behaviour and biodistribution of the radiopharmaceutical *in vivo*, and a unique balance must be made between all components. In this regard, it is difficult to introduce the radiometal and BFC onto the biomolecule without hindering the targeting ability of the biovector. Moreover, *in vitro* and *in vivo* evaluation methods for bioconjugates varies throughout the literature and it can be difficult to compare results across different studies. Caution should also be taken when analysing biodistribution data that have been extracted from small animal models, promising results there do not always translate well to human patients.

The array of antigens being targeted by radiometallated bioconjugates covers a broad spectrum of human cancers, with some being over-expressed in multiple cancer types thus expanding their applicability in the clinic. The infinite number of metal–chelate–linker–biomolecule combinations available to the radiochemist indicate the field of radiopharmaceuticals has the potential to be widely used providing diagnosis and treatment catered to individual patients.

## Concluding remarks

Radiometals in nuclear oncology encompass a wide range of  $\gamma$  and  $\beta^+$  emitters for imaging with SPECT and PET respectively, and  $\alpha$ ,  $\beta^-$ , and Auger electron emitters for therapy, some of which have been successfully incorporated into FDA-approved radiopharmaceuticals. Radiometals possess a number of advantages over traditional ‘organic’ radioisotopes: an array of possible emissions and half-lives that span a range needed to ask and answer those questions researchers and clinicians want to address while also being able to match biological and radiological half-lives, and the ability to introduce the radionuclide through quick and convenient coordination bonds *via* the BFC method. The modular assembly of the BFC method allows for a vast and quickly advancing field of treatments that

are patient specific. With new biomarkers, radiometals, and chelating strategies available, there is now a plethora of combinations available for radiopharmaceutical design.

Despite the FDA-approval of a few successful metal-based radiopharmaceuticals for SPECT imaging and  $\beta^-$  therapy in the last decade, there is still no radiometal-based PET imaging agent, or radiotherapeutic agent of  $\alpha$  or Auger electron emitters on the market. In part, the standard regulatory and financial barriers slow new metallo-radiopharmaceuticals from entering the clinic. As new cost-efficient methods for the production and wide-spread distribution of these radiometals are developed, new agents will undoubtedly be produced that demonstrate value to the clinician and patient and these barriers will slowly diminish, turning these once entitled ‘non-traditional’ isotopes into standard convention.

## Acknowledgements

Acknowledgement is made to the Natural Sciences and Engineering Research Council (NSERC) of Canada for Discovery and Collaborative Research and Development (CRD) grants, to Nordion for isotopes and support, to UBC for a four-year fellowship (C.F.R) and NSERC CGSD (C.F.R) for funding, to the Canada Council for the Arts for a Killam Research Fellowship (C.O. 2011–2013), and to Eric Price and Dr Jacqueline Cawthray for thoughtful discussion and editing.

## Notes and references

- 1 Cancer Fact Sheet No. 297 – World Health Organization, 2012.
- 2 P. W. Miller, N. J. Long, R. Vilar and A. D. Gee, *Angew. Chem., Int. Ed.*, 2008, **47**, 8998–9033.
- 3 List of FDA-approved radiopharmaceuticals v. 8 – Cardinal Health, 2012; www.cardinal.com, accessed December 15, 2012.
- 4 C. Bolzati, F. Refosco, A. Marchiani and P. Ruzza, *Curr. Med. Chem.*, 2010, **17**, 2656–2683.
- 5 S. Liu and S. Chakraborty, *Dalton Trans.*, 2011, **40**, 6077–6086.
- 6 S. Bhattacharyya and M. Dixit, *Dalton Trans.*, 2011, **40**, 6112–6128.
- 7 J. P. Holland, M. J. Williamson and J. S. Lewis, *Mol. Imaging*, 2010, **9**, 1–20.
- 8 T. J. Wadas, E. H. Wong, G. R. Weisman and C. J. Anderson, *Chem. Rev.*, 2010, **110**, 2858–2902.
- 9 S. V Smith, *J. Inorg. Biochem.*, 2004, **98**, 1874–1901.
- 10 C. M. Gomes, A. J. Abrunhosa, P. Ramos and E. K. J. Pauwels, *Adv. Drug Delivery Rev.*, 2011, **63**, 547–554.
- 11 I. Verel, G. W. M. Visser and G. A. van Dongen, *J. Nucl. Med.*, 2005, **46**(suppl. 1), 164S–171S.
- 12 B. N. Ganguly, N. N. Mondal, M. Nandy and F. Roesch, *J. Radioanal. Nucl. Chem.*, 2009, **279**, 685–698.
- 13 B. M. Zeglis and J. S. Lewis, *Dalton Trans.*, 2011, **40**, 6168–6195.
- 14 W. A. Volkert, W. F. Goeckeler, G. J. Ehrhardt and A. R. Ketring, *J. Nucl. Med.*, 1991, **32**, 174–185.
- 15 C. A. Boswell and M. W. Brechbiel, *Nucl. Med. Biol.*, 2007, **34**, 757–778.
- 16 G. Vaidyanathan and M. R. Zalutsky, *Phys. Med. Biol.*, 1996, **41**, 1915–1931.
- 17 J. A. O'Donoghue and T. E. Wheldon, *Phys. Med. Biol.*, 1996, **41**, 1973–1992.
- 18 C. A. Boswell and M. W. Brechbiel, *J. Nucl. Med.*, 2005, **46**, 1946–1947.
- 19 S. S. Jurisson and J. D. Lydon, *Chem. Rev.*, 1999, **99**, 2205–2218.
- 20 A. L. Våvere and J. S. Lewis, *Dalton Trans.*, 2007, 4893–4902.
- 21 J. L. J. Dearling and A. B. Packard, *Nucl. Med. Biol.*, 2010, **37**, 237–243.
- 22 W. R. Harris, *Struct. Bonding*, 1998, **92**, 121–162.

- 23 H. Sun, M. C. Cox, H. Li and P. J. Sadler, *Struct. Bonding*, 1997, **88**, 72–102.
- 24 C. J. Anderson and M. J. Welch, *Chem. Rev.*, 1999, **99**, 2219–2234.
- 25 S. M. Qaim, *Q. J. Nucl. Med. Mol. Imaging*, 2008, **52**, 111–120.
- 26 P. J. Blower, J. S. Lewis and J. Zweit, *Nucl. Med. Biol.*, 1996, **23**, 957–980.
- 27 www.ClinicalTrials.gov, accessed December 13, 2012.
- 28 M. Shokeen and T. J. Wadas, *Med. Chem.*, 2011, **7**, 413–429.
- 29 R. Shannon, *Acta Crystallogr., Sect. A: Cryst. Phys., Diff., Theor. Gen. Crystallogr.*, 1976, **32**, 751–767.
- 30 M. D. Bartholomä, *Inorg. Chim. Acta*, 2012, **389**, 36–51.
- 31 M. Fani, J. P. Andre and H. R. Maecke, *Contrast Media Mol. Imaging*, 2008, **3**, 53–63.
- 32 L. R. Perk, G. W. M. Visser, M. J. W. D. Vosjan, M. S. Walsum, B. M. Tjink, C. Rene and G. A. M. S. Van Dongen, *J. Nucl. Med.*, 2005, **46**, 1898–1906.
- 33 M. A. Deri, B. M. Zeglis, L. C. Francesconi and J. S. Lewis, *Nucl. Med. Biol.*, 2013, **40**, 3–14.
- 34 D. S. Abou, T. Ku and P. M. Smith-Jones, *Nucl. Med. Biol.*, 2011, **38**, 675–681.
- 35 S. Liu, *Adv. Drug Delivery Rev.*, 2008, **60**, 1347–1370.
- 36 C. S. Cutler, H. M. Hennkens, N. Sisay, S. Huclier-Markai and S. S. Jurisson, *Chem. Rev.*, 2013, **113**, 858–883.
- 37 P. S. Donnelly, *Dalton Trans.*, 2011, **40**, 999–1010.
- 38 U. Schötz, H. Schrader, E. Schönfeld, E. Günther and R. Klein, *Appl. Radiat. Isot.*, 2001, **55**, 89–96.
- 39 M. L. Bowen and C. Orvig, *Chem. Commun.*, 2008, 5077–5091.
- 40 O. Couturier, S. Supiot, M. Degraef-Mougin, A. Faivre-Chauvet, T. Carlier, J.-F. Chatal, F. Davodeau and M. Cherel, *Eur. J. Nucl. Med. Mol. Imaging*, 2005, **32**, 601–614.
- 41 M. Miederer, D. A. Scheinberg and M. R. McDevitt, *Adv. Drug Delivery Rev.*, 2008, **60**, 1371–1382.
- 42 M. McDevitt, D. Ma, J. Simon, R. K. Frank and D. A. Scheinberg, *Appl. Radiat. Isot.*, 2002, **57**, 841–847.
- 43 L. L. Chappell, K. A. Deal, E. Dadachova and M. W. Brechbiel, *Bioconjugate Chem.*, 2000, **11**, 510–519.
- 44 A. M. E. Gustafsson, T. Bäck, J. Elgqvist, L. Jacobsson, R. Hultborn, P. Albertsson, A. Morgenstern, F. Bruchertseifer, H. Jensen and S. Lindgren, *Nucl. Med. Biol.*, 2012, **39**, 15–22.
- 45 T. L. Rosenblat, M. R. McDevitt, D. a Mulford, N. Pandit-Taskar, C. R. Divgi, K. S. Panageas, M. L. Heaney, S. Chandel, A. Morgenstern, G. Sgouras, S. M. Larson, D. A. Scheinberg and J. G. Jurcic, *Clin. Cancer Res.*, 2010, **16**, 5303–5311.
- 46 S. Hassfjell and M. W. Brechbiel, *Chem. Rev.*, 2001, **101**, 2019–2036.
- 47 M. W. Brechbiel, O. A. Gansow, C. G. Pippin, R. D. Rogers and R. P. Planalp, *Inorg. Chem.*, 1996, **35**, 6343–6348.
- 48 K. Yong and M. W. Brechbiel, *Dalton Trans.*, 2011, **40**, 6068–6076.
- 49 L. L. Chappell, E. Dadachova, D. E. Milenic, K. Garmestani, C. Wu and M. W. Brechbiel, *Nucl. Med. Biol.*, 2000, **27**, 93–100.
- 50 D. E. Milenic, E. D. Brady and M. W. Brechbiel, *Nat. Rev. Drug Discovery*, 2004, **3**, 488–499.
- 51 D. Ma, M. R. McDevitt, R. D. Finn and D. A. Scheinberg, *Appl. Radiat. Isot.*, 2001, **55**, 667–678.
- 52 E. W. Price, J. F. Cawthray, G. Bailey, C. L. Ferreira, E. Boros, M. J. Adam and C. Orvig, *J. Am. Chem. Soc.*, 2012, **134**, 8670–8683.
- 53 E. Boros, C. L. Ferreira, J. F. Cawthray, E. W. Price, B. O. Patrick, D. W. Wester, M. J. Adam and C. Orvig, *J. Am. Chem. Soc.*, 2010, **132**, 15726–15733.
- 54 A. J. Chang, R. A. De Silva and S. E. Lapi, *Mol. Imaging*, 2013, **12**, 17–27.
- 55 J. D. G. Correia, A. Paulo, P. D. Raposo and I. Santos, *Dalton Trans.*, 2011, **40**, 6144–6167.
- 56 A. S. Craig, D. Parker, H. Adams and N. A. Bailey, *J. Chem. Soc., Chem. Commun.*, 1989, 1793–1794.
- 57 I. U. Khan and A. G. Beck-Sickinger, *Anti-Cancer Agents Med. Chem.*, 2008, **8**, 186–199.
- 58 G. Tircsó, E. T. Benyó, E. H. Suh, P. Jurek, G. E. Kiefer, A. D. Sherry and Z. Kovács, *Bioconjugate Chem.*, 2009, **20**, 565–575.
- 59 C. L. Ferreira, E. Lamsa, M. Woods, Y. Duan, P. Fernando, C. Bensimon, M. Kordos, K. Guenther, P. Jurek and G. E. Kiefer, *Bioconjugate Chem.*, 2010, **21**, 531–536.
- 60 C. L. Ferreira, D. T. Yapp, E. Lamsa, M. Gleave, C. Bensimon, P. Jurek and G. E. Kiefer, *Nucl. Med. Biol.*, 2008, **35**, 875–882.
- 61 J. Notni, P. Hermann, J. Havlicková, J. Kotek, V. Kubiček, J. Plutnar, N. Loktionova, P. J. Riss, F. Rösch and I. Lukeš, *Chem.-Eur. J.*, 2010, **16**, 7174–7185.
- 62 J. Notni, J. Šimeček, P. Hermann and H.-J. Wester, *Chem.-Eur. J.*, 2011, **17**, 14718–14722.
- 63 C. A. Boswell, C. A. S. Regino, K. E. Baidoo, K. J. Wong, A. Bumb, H. Xu, D. E. Milenic, J. A. Kelley, C. C. Lai and M. W. Brechbiel, *Bioconjugate Chem.*, 2008, **19**, 1476–1484.
- 64 V. Maheshwari, J. L. J. Dearling, S. T. Treves and A. B. Packard, *Inorg. Chim. Acta*, 2012, **393**, 318–323.
- 65 M. S. Cooper, M. T. Ma, K. Sunassee, K. P. Shaw, J. D. Williams, R. L. Paul, P. S. Donnelly and P. J. Blower, *Bioconjugate Chem.*, 2012, **23**, 1029–1039.
- 66 K. A. Deal, I. A. Davis, S. Mirzadeh, S. J. Kennel and M. W. Brechbiel, *J. Med. Chem.*, 1999, **42**, 2988–2992.
- 67 C. Wängler, R. Schirrmacher, P. Bartenstein and B. Wängler, *Curr. Med. Chem.*, 2010, **17**, 1092–1116.
- 68 A. Y. Lebedev, J. P. Holland and J. S. Lewis, *Chem. Commun.*, 2010, **46**, 1706–1708.
- 69 G. A. Bailey, E. W. Price, B. M. Zeglis, C. L. Ferreira, E. Boros, M. J. Lacasse, B. O. Patrick, J. S. Lewis, M. J. Adam and C. Orvig, *Inorg. Chem.*, 2012, **51**, 12575–12589.
- 70 H. Struthers, B. Spingler, T. L. Mindt and R. Schibli, *Chem.-Eur. J.*, 2008, **14**, 6173–6183.
- 71 D. Hanahan and R. A. Weinberg, *Cell*, 2000, **100**, 57–70.
- 72 S. Ciavarella, A. Milano, F. Dammacco and F. Silvestris, *Biodrugs*, 2010, **24**, 77–88.
- 73 D. Denoyer, N. Perek, N. Le Jeune and F. Dubois, *Curr. Cancer Drug Targets*, 2006, **6**, 181–196.
- 74 G. Ting, C. Chang and H. Wang, *Anticancer Res.*, 2009, **29**, 4107–4118.
- 75 M. Hamoudeh, M. A. Kamleh, R. Diab and H. Fessi, *Adv. Drug Delivery Rev.*, 2008, **60**, 1329–1346.
- 76 E. C. F. Dijkers, J. G. W. Kosterink, A. P. Rademaker, L. R. Perk, G. A. M. S. van Dongen, J. Bart, J. R. de Jong, E. G. E. de Vries and M. N. Lub-de Hooge, *J. Nucl. Med.*, 2009, **50**, 974–981.
- 77 P. Ruzza and A. Calderan, *Expert Opin. Med. Diagn.*, 2011, **5**, 411–424.
- 78 A. J. de Graaf, M. Kooijman, W. E. Hennink and E. Mastrobattista, *Bioconjugate Chem.*, 2009, **20**, 1281–1295.
- 79 M. Langer and A. G. Beck-Sickinger, *Curr. Med. Chem.: Anti-Cancer Agents*, 2001, **1**, 71–93.
- 80 C. K. Younes, R. Boisgard and B. Tavittian, *Curr. Pharm. Des.*, 2002, **8**, 1451–1466.
- 81 T. Olafsen and A. M. Wu, *Semin. Nucl. Med.*, 2010, **40**, 167–181.
- 82 S. M. Knowles and A. M. Wu, *J. Clin. Oncol.*, 2012, **30**, 3884–3892.
- 83 S. Hoppmann, S. Qi, Z. Miao, H. Liu, H. Jiang, C. S. Cutler, A. Bao and Z. Cheng, *JBIC, J. Biol. Inorg. Chem.*, 2012, **17**, 709–718.
- 84 P. M. Smith-Jones, D. B. Solit, T. Akhurst, F. Afroze, N. Rosen and S. M. Larson, *Nat. Biotechnol.*, 2004, **22**, 701–706.
- 85 M. J. Welch, C. J. Hawker and K. L. Wooley, *J. Nucl. Med.*, 2009, **50**, 1743–1746.
- 86 M. Fani and H. R. Maecke, *Eur. J. Nucl. Med. Mol. Imaging*, 2012, **39**(suppl. 1), S11–S30.
- 87 E. Benedetti, G. Morelli, A. Accardo, R. Mansi, D. Tesaro and L. Aloj, *Biodrugs*, 2004, **18**, 279–295.
- 88 K. P. Koopmans and A. W. J. M. Glaudemans, *Eur. J. Nucl. Med. Mol. Imaging*, 2012, **39**(suppl. 1), S4–S10.
- 89 H. R. Maecke, M. Hofmann and U. Haberkorn, *J. Nucl. Med.*, 2005, **46**, 172–178.
- 90 F. C. Gaertner, H. Kessler, H.-J. Wester, M. Schwaiger and A. J. Beer, *Eur. J. Nucl. Med. Mol. Imaging*, 2012, **39**(suppl. 1), S126–S138.
- 91 J.-H. Kim, J.-C. Lim, K.-C. Yun, S.-J. Choi and Y.-D. Hong, *J. Labelled Compd. Radiopharm.*, 2012, **55**, 10–17.
- 92 T. J. Wadas, H. Deng, J. E. Sprague, A. Zheleznyak, K. N. Weilbaecher and C. J. Anderson, *J. Nucl. Med.*, 2009, **50**, 1873–1880.
- 93 J. Shi, Y.-S. Kim, S. Chakraborty, Y. Zhou, F. Wang and S. Liu, *Amino Acids*, 2011, **41**, 1059–1070.
- 94 M. T. Ma, O. C. Neels, D. Denoyer, P. Roselt, J. A. Karas, D. B. Scanlon, J. M. White, R. J. Hicks and P. S. Donnelly, *Bioconjugate Chem.*, 2011, **22**, 2093–2103.
- 95 Z. Liu, J. Shi, B. Jia, Z. Yu, Y. Liu, H. Zhao, F. Li, J. Tian, X. Chen, S. Liu and F. Wang, *Mol. Pharmaceutics*, 2011, **8**, 591–599.
- 96 M. Jiang, R. Ferdani, M. Shokeen and C. J. Anderson, *Nucl. Med. Biol.*, 2013, **40**, 245–251.
- 97 D. Shetty, Y.-S. Lee and J. M. Jeong, *Nucl. Med. Mol. Imaging*, 2010, **44**, 233–240.

- 98 L. Wei, X. Zhang, F. Gallazzi, Y. Miao, X. Jin, M. W. Brechbiel, H. Xu, T. Clifford, M. J. Welch, J. S. Lewis and T. P. Quinn, *Nucl. Med. Biol.*, 2009, **36**, 345–354.
- 99 Y. Miao, T. J. Hoffman and T. P. Quinn, *Nucl. Med. Biol.*, 2005, **32**, 485–493.
- 100 M. T. Ma and P. S. Donnelly, *Curr. Top. Med. Chem.*, 2011, **11**, 500–520.
- 101 R. Mansi, X. Wang, F. Forrer, B. Waser, R. Cescato, K. Graham, S. Borkowski, J. C. Reubi and H. R. Maecke, *Eur. J. Nucl. Med. Mol. Imaging*, 2011, **38**, 97–107.
- 102 D. L. Costantini, D. F. Villani, K. a Vallis and R. M. Reilly, *J. Nucl. Med.*, 2010, **51**, 477–483.
- 103 J. P. Norenberg, B. J. Krenning, I. R. H. M. Konings, D. F. Kusewitt, T. K. Nayak, T. L. Anderson, M. de Jong, K. Garmestani, M. W. Brechbiel and L. K. Kvols, *Clin. Cancer Res.*, 2006, **12**, 897–903.
- 104 M. T. Ma, M. S. Cooper, R. L. Paul, K. P. Shaw, J. A. Karas, D. Scanlon, J. M. White, P. J. Blower and P. S. Donnelly, *Inorg. Chem.*, 2011, **50**, 6701–6710.
- 105 Z. Cheng, J. Chen, Y. Miao, N. K. Owen, T. P. Quinn and S. S. Jurisson, *J. Med. Chem.*, 2002, **45**, 3048–3056.
- 106 S. Roosenburg, P. Laverman, L. Joosten, A. Eek, W. J. G. Oyen, M. de Jong, F. P. J. T. Rutjes, F. L. van Delft and O. C. Boerman, *Bioconjugate Chem.*, 2010, **21**, 663–670.
- 107 I. Velikyan, A. L. Sundberg, O. Lindhe, A. U. Höglund, O. Eriksson, E. Werner, J. Carlsson, M. Bergström, B. Långström and V. Tolmachev, *J. Nucl. Med.*, 2005, **46**, 1881–1888.
- 108 T. K. Nayak, K. Garmestani, K. E. Baidoo, D. E. Milenic and M. W. Brechbiel, *Int. J. Cancer*, 2011, **128**, 920–926.